DTP-99-67
KCL-MTH-99-39
ITFA 99-26
hep-th/9909216
September 29, 1999

g-function flow in perturbed boundary conformal field theories

Patrick Dorey[1], Ingo Runkel[2], Roberto Tateo[3] and Gérard Watts[4]

[1]*Department of Mathematical Sciences,*
University of Durham, Durham DH1 3LE, England

[3]*Universiteit van Amsterdam, Inst. voor Theoretische Fysica*
1018 XE Amsterdam, The Netherlands

[2,4]*Mathematics Department,*
King's College London, Strand, London WC2R 2LS, U.K.

Abstract

The g-function was introduced by Affleck and Ludwig as a measure of the ground state degeneracy of a conformal boundary condition. We consider this function for perturbations of the conformal Yang–Lee model by bulk and boundary fields using conformal perturbation theory (CPT), the truncated conformal space approach (TCSA) and the thermodynamic Bethe Ansatz (TBA). We find that the TBA equations derived by LeClair et al describe the massless boundary flows, up to an overall constant, but are incorrect when one considers a simultaneous bulk perturbation; however the TBA equations do correctly give the 'non-universal' linear term in the massive case, and the ratio of g-functions for different boundary conditions is also correctly produced. This ratio is related to the Y–system of the Yang–Lee model and by comparing the perturbative expansions of the Y–system and of the g-functions we obtain the exact relation between the UV and IR parameters of the massless perturbed boundary model.

[1]e-mail: P.E.Dorey@durham.ac.uk
[2]e-mail: ingo@mth.kcl.ac.uk
[3]e-mail: tateo@wins.uva.nl
[4]e-mail: gmtw@mth.kcl.ac.uk

1 Introduction

Consider the partition function of a classical statistical-mechanical system defined on a cylinder of length R and circumference L. Among the characteristics of the model might be a bulk mass scale M and boundary scales depending on the boundary conditions α and β imposed at the two ends of the cylinder; we will highlight the role of these quantities by denoting the partition function $Z_{\alpha\beta}(M, R, L)$. If R is taken to infinity with all other variables held fixed, then

$$Z_{\alpha\beta}(M, R, L) \sim A_{\alpha\beta}(M, L)\, \mathrm{e}^{-R\, E_0^{\mathrm{circ}}(M,L)} \ , \tag{1.1}$$

where $E_0^{\mathrm{circ}}(M, L)$ is the ground state energy of the model on a circle of circumference L. To derive this asymptotic R-dependence, it is sufficient to treat the boundary conditions as boundary states $|\, \alpha \,\rangle$ [1] in a formalism where time runs along the length of the cylinder, and states are propagated by a bulk Hamiltonian $H_{\mathrm{circ}}(M, L)$:

$$Z_{\alpha\beta}(M, R, L) = \langle\, \alpha \,|\, \exp(-R H_{\mathrm{circ}}(M, L)) \,|\, \beta \,\rangle \ . \tag{1.2}$$

At large R the contribution of the ground state $|\, \Omega \,\rangle$ dominates, establishing (1.1) and also giving

$$A_{\alpha\beta}(M, L) = \frac{\langle\, \alpha \,|\, \Omega \,\rangle \, \langle\, \Omega \,|\, \beta \,\rangle}{\langle\, \Omega \,|\, \Omega \,\rangle} \ . \tag{1.3}$$

The inner products appearing in (1.3) should in general contain a term corresponding to a free-energy per unit length, i.e.

$$\log\Big(\frac{\langle\, \Omega \,|\, \alpha \,\rangle}{\langle\, \Omega \,|\, \Omega \,\rangle^{1/2}} \Big) = -L f_\alpha + \log(g_\alpha(M, L)) \ . \tag{1.4}$$

This linear term can in principle be extracted unambiguously from the large L behaviour of $\log(\, \langle\, \Omega \,|\, \alpha \,\rangle\,)$. The question is then whether the functions $\log(g_\alpha(M, L))$ now contain universal information.

In the case $M = 0$, i.e. for critical bulk, Affleck and Ludwig [2] pointed out that the UV and IR limits of these functions, $\log(g_\alpha(0, 0))$ and $\log(g_\alpha(0, \infty))$, play the role of a generalised ground state degeneracy for the UV and IR conformal boundary conditions respectively. These can be easily calculated for many conformal field theories, and can enable one to identify the boundary conditions uniquely.

The universality of the g-functions is however a somewhat delicate issue when the model has a mass scale, either in the bulk or at the boundary. For example, one could imagine that in some calculational schemes the boundaries acquire a finite thickness, and so the effective cylinder length would decrease by some finite amount δ to $R - \delta$, in which case $\log(g_\alpha)$ would be altered

$$\log(g_\alpha(M, L)) \to \log(g_\alpha(M, L)) + \frac{\pi\delta}{12L} c(ML) \ , \tag{1.5}$$

where $c(ML)$ is related to the ground state energy on the circle by

$$E_0^{\mathrm{circ}}(M, L) = f_{\mathrm{bulk}} L - \frac{\pi}{6L} c(ML) \ . \tag{1.6}$$

More generally, the fact that the g-functions have to be extracted from subleading contributions to $\log Z$ makes their calculation much trickier than that of the corresponding bulk quantity $c(ML)$.

If the model is integrable, one might hope to be able to address these issues in greater depth. This was one of the topics of some work by LeClair et al. [3]. Using the thermodynamic Bethe ansatz (TBA) technique, they proposed equations for $\log(g)$, but up to now these have not been checked in detail. The main purpose of this paper is to provide some such checks in a concrete example, namely the scaling Yang-Lee model, making use both of conformal perturbation theory and of a recently-introduced generalisation of the TCSA to boundary situations [4]. We find that the TBA g-functions describes the *massless* flow well (up to an overall constant) but the *massive* flows are not well described. However, we find that the TBA g-functions of [3] do appear to describe correctly the *ratio* of the g-functions for different boundary conditions of the same bulk model. Further, the TBA expression for this ratio has a very simple form in terms of the Y–function of the Yang–Lee model. This enables us to (a) provide a perturbative expansion for the massive Y–function and (b) find the coefficient in the relation between UV and IR parameters in the boundary Yang-Lee model model exactly, a result announced in [4].

We first discuss the conformal perturbation theory (CPT) expressions for $\log g$ and then how the truncated conformal space approach (TCSA) can be used to investigate these functions. We then turn to the TBA equations and the properties of their solutions. Finally we compare the results of the two methods and find the relation between UV and IR parameters.

2 Boundary conformal field theory

We begin with a sketch of boundary conformal field theory in general, although we shall often specialise to those theories described in the bulk by a minimal Virasoro theories with 'A'–type diagonal modular invariant. At the end we give the details for the Yang-Lee model. For a general discussion of the boundary content of the Virasoro minimal models see [5].

A boundary conformal field theory is specified by giving the field content in the bulk, a list of the possible boundary conditions and the field contents of these boundary conditions, the fields which interpolate them, and some constants.

In the bulk there are primary fields Φ_i of weights $h_i, \overline{h}_i$ which for a diagonal modular invariant are equal; under conformal transformations they obey

$$\Phi_i(z,\overline{z}) = \left|\frac{\partial w}{\partial z}\right|^{x_i} \Phi_i(w,\overline{w}) \ ,$$

where $x_i = 2h_i$.

For the A–series, the conformal boundary conditions (which we shall denote by α) may themselves also be indexed by the Virasoro minimal representations [1, 5]. We adopt the notation $\phi_j^{(\alpha\beta)}(x)$ for a field of weight h_j which interpolates two boundary conditions α, β, which may be the same or different. Such a field exists if the fusion coefficient $N_{\alpha\,\beta}{}^{i}$ is one, and does not exist if it is zero*. We take such boundary primary fields to transform under

*Remember that for A-modular invariant Virasoro minimal models all representations are self-conjugate and all the fusion coefficients are either 1 or 0

conformal transformations as[†]

$$\phi_i^{(\alpha\beta)}(z) = \left|\frac{\partial w}{\partial z}\right|^{h_i} \phi_i^{(\alpha\beta)}(w) \ .$$

Inside correlation functions we assume that the product of fields can be replaced by their operator product expansion – we do not try to interpret them as genuine expansions of the actions of operators, nor do we consider the associated problems of orderings of the arguments of the fields.

There are three different operator products – bulk-bulk, bulk-boundary and boundary-boundary. The first are the standard expressions[‡] ,

$$\Phi_i(z,\overline{z})\,\Phi_j(w,\overline{w}) \sim \sum_k C_{ij}{}^k\,|z-w|^{x_k-x_i-x_j}\ \Phi_k(w,\overline{w}) + \dots \ . \tag{2.1}$$

Next we have the operator products of the boundary primary fields:

$$\phi_i^{(\alpha\beta)}(z)\,\phi_j^{(\beta\gamma)}(w) \sim \sum_k c_{ij}^{(\alpha\beta\gamma)k}\ |z-w|^{h_k-h_i-h_j}\ \phi_k^{(\alpha\gamma)}(w) + \dots \ . \tag{2.2}$$

Finally, a primary bulk field near a boundary of type α may be expanded in boundary fields as

$$\Phi_i(z,\overline{z}) \sim \sum_j {}^{(\alpha)}B_i^j\,|2(z-w)|^{h_j-x_i}\,\phi_j^{(\alpha\alpha)}(w) + \dots \ , \tag{2.3}$$

where z is in the bulk and w is the point on the boundary closest to z.

To determine the correlation functions consistently, one needs to normalise the different boundary conditions differently. One way to do this is to give the zero-point functions on a disc of radius 1 with boundary condition α, which we denote by Z_α,

$$Z_\alpha = \langle\, 1\,\rangle_\alpha^{\rm disc} \ . \tag{2.4}$$

The rules for calculating the various constants in equations (2.1), (2.2), (2.3) and (2.4) are essentially given in a series of papers by Cardy and Lewellen [1,7,8], but some work is required to obtain explicit expressions. For the structure constants of the A–type model, see [9].

Using these structure constants, zero-point functions and the chiral blocks, we can assign a value to any n-point function, i.e. to any surface with some assignment of conformal boundary conditions to the boundaries, and some insertions of bulk and boundary fields; if the boundary conditions change at some point along a boundary, then there is of necessity a boundary changing field inserted at this point.

We can now express various simple correlation functions on a disc of radius 1 in terms of

[†]There is some choice in the transformations of boundary fields, see [6]

[‡]n.b. in the 'A'-type invariant we only have spinless bulk primary fields

these structure constants:

$$\begin{aligned}
\Big\langle\, \phi_i^{(\alpha\alpha)}(e^{i\theta}) \,\Big\rangle_\alpha^{\rm disc} &= 0\ , \qquad\qquad \langle\ 1\ \rangle_\alpha^{\rm disc} \ = \ Z_\alpha \\
\langle\, \Phi_i(z,\overline{z}) \,\rangle_\alpha^{\rm disc} &= \left({}^{(\alpha)}B_i^1\, Z_\alpha \right)\ (1-|z|^2)^{-x_i}\ , \\
\Big\langle\, \Phi_i(re^{i\theta})\ \phi_j^{(\alpha\alpha)}(1) \,\Big\rangle_\alpha^{\rm disc} &= \left({}^{(\alpha)}B_i^j\, c_{jj}^{(\alpha\alpha\alpha)1}\, Z_\alpha \right)\ \left|1-2r\cos\theta+r^2\right|^{-h_j}\ \left|1-r^2\right|^{h_j-x_i}\ , \\
\Big\langle\, \phi_i^{(\alpha\beta)}(\theta_1)\ \phi_i^{(\beta\alpha)}(\theta_2) \,\Big\rangle^{\rm disc} &= \left(c_{ii}^{(\alpha\beta\alpha)1}\, Z_\alpha \right)\ \left|2\sin\tfrac{\theta_{12}}{2}\right|^{-2h_i}\ , \\
\Big\langle\, \phi_i^{(\alpha\beta)}(\theta_1)\ \phi_j^{(\beta\gamma)}(\theta_2)\ \phi_k^{(\gamma\alpha)}(\theta_3) \,\Big\rangle^{\rm disc} &= \left(c_{ij}^{(\alpha\beta\gamma)k}\, c_{kk}^{(\alpha\gamma\alpha)1}\, Z_\alpha \right) \\
&\times\ \left|2\sin\tfrac{\theta_{12}}{2}\right|^{h_k-h_i-h_j} \left|2\sin\tfrac{\theta_{23}}{2}\right|^{h_i-h_j-h_k} \left|2\sin\tfrac{\theta_{13}}{2}\right|^{h_j-h_k-h_i}\ ,
\end{aligned} \tag{2.5}$$

where $\theta_{ij} = \theta_i - \theta_j$, etc.

We are interested in calculating correlation functions on the cylinder but we will be able to relate all the quantities of interest to simpler correlation functions on a disc.

Let us consider the partition function of a right cylinder of length R, with the two ends being circles of circumference L with conformal boundary conditions α and β. This can be realised as a rectangle in the upper half plane with vertices 0, L, iR and $L+iR$, with the two vertical sides identified. The partition function can be written as

$$Z_{(\alpha\beta)}^{\rm cyl}(R,L) = {\rm Tr}_{\mathcal{H}_{(\alpha\beta)}} \left(\exp(-L\widehat{H}_{(\alpha\beta)}^{\rm strip}(R)) \right)\ . \tag{2.6}$$

By mapping this rectangle to a half-annulus in the upper half plane by $z \mapsto \exp(\pi z/R)$, we can use the operator formalism in the upper-half plane. The Hilbert space $\mathcal{H}_{(\alpha\beta)}$ decomposes into a direct sum of irreducible representations of one copy of the Virasoro algebra

$$\mathcal{H}_{(\alpha\beta)} = \oplus_i\, N_{(\alpha\beta)}{}^i\, \mathcal{H}_i\ , \tag{2.7}$$

and the Hamiltonian is given as

$$\widehat{H}_{(\alpha\beta)}^{\rm strip} = \frac{\pi}{R}(L_0 - \frac{c}{24})\ , \tag{2.8}$$

so that

$$Z_{(\alpha\beta)}^{\rm cyl}(R,L) = \sum_i\, N_{\alpha\beta}{}^i\, \chi_i(q)\ , \tag{2.9}$$

where $\chi_i(q)$ is the character of the representation i, $q = \exp(-\pi L/R)$, and $N_{\alpha\beta}{}^i$ are the Verlinde fusion numbers.

We can also map the cylinder into a complete annulus of inner and outer radii $\exp(-2\pi R/L)$ and 1 respectively by $z{\mapsto}w{=}\exp(2i\pi z/L)$, and use the operator formalism on the plane. The Hilbert space for the bulk theory on the plane carries a representation of two copies of the Virasoro algebra, in terms of which the cylinder Hamiltonian is given as

$$\widehat{H}^{\rm circ} = \frac{2\pi}{L}(L_0 + \overline{L}_0 - \frac{c}{12})\ . \tag{2.10}$$

This space carries a representation of two copies of the Virasoro algebra. The highest weight states $|\,i\,\rangle$ are labelled by the highest weight representations of the Virasoro algebra and given by the action of the bulk primary fields on the $SL(2)$–invariant vacuum $|\,0\,\rangle$ by

$$|\,i\,\rangle = \lim_{w\to 0} \Phi_i(w,\overline{w})\,|\,0\,\rangle\ , \tag{2.11}$$

and hence

$$\langle\, i\,|\,j\,\rangle = \delta_{ij}\, C_{ii}{}^{1}\,\langle\, 0\,|\,0\,\rangle\ .$$

We shall not necessarily normalise the vacuum to be norm 1, and indeed for the Yang-Lee model it is convenient to take $\langle\, 0\,|\,0\,\rangle = -1$.

The partition function on the cylinder can be calculated in terms of boundary states $|\,\alpha\,\rangle$, $|\,\beta\,\rangle$ in the Hilbert space for the bulk theory on the plane:

$$Z^{\rm cyl}_{\alpha\beta} = \langle\,\alpha\,|\,e^{-R\widehat{H}^{\rm circ}(L)}\,|\,\beta\,\rangle\ . \tag{2.12}$$

For a boundary state to represent a circular boundary with conformally invariant boundary condition, it must satisfy

$$\big(L_m - \overline{L}_{-m}\big)\,|\,\alpha\,\rangle = 0\ ,\quad \langle\,\alpha\,|\,\big(L_m - \overline{L}_{-m}\big) = 0\ .$$

A basis of states satisfying these conditions are the Ishibashi states. There is one such state for each Virasoro representation in the minimal model in question, which we denote by

$$|\,i\,\rangle\!\rangle = \left\{1 + \frac{L_{-1}\overline{L}_{-1}}{2h_i} + \ldots\right\}|i\rangle\ ,\quad |\,0\,\rangle\!\rangle = \left\{1 + \frac{L_{-2}\overline{L}_{-2}}{c/2} + \ldots\right\}|0\rangle\ .$$

$$\langle\!\langle\, i\,| = \langle\, i\,|\left\{1 + \frac{L_1\overline{L}_1}{2h_i} + \ldots\right\}\ ,\quad \langle\!\langle\, 0\,| = \langle\, 0\,|\left\{1 + \frac{L_2\overline{L}_2}{c/2} + \ldots\right\}\ .$$

These are normalised so that

$$\langle\!\langle\, i\,|\,e^{-R\widehat{H}^{\rm circ}(L)}\,|\,j\,\rangle\!\rangle = \delta_{ij}\,\chi_i(\widetilde{q})\,\langle\, i\,|\,i\,\rangle\ ,$$

where $\widetilde{q} = \exp(-4\pi R/L)$. We expand the boundary states in terms of the Ishibashi states as

$$|\,\alpha\,\rangle = \sum_j g^j_\alpha\,|\,j\,\rangle\!\rangle\ .$$

(It is always possible to normalise the fields and states such that the coefficients g^i_α are real, and we shall assume that has been done. See [9] for details). Using these states, the partition function is given from (2.12) by

$$Z^{\rm cyl}_{(\alpha\beta)}(r_1,r_2) \;=\; \sum_i g^i_\alpha\, g^i_\beta\,\chi_i(\widetilde{q})\,\langle\, i\,|\,i\,\rangle\ . \tag{2.13}$$

Noting that

$$Z^{\rm cyl}_{\alpha\beta} = \sum_{ij} N^i_{\alpha\beta}\, S_i{}^j\,\chi_j(\widetilde{q})\ ,$$

where $S_i{}^j$ is the matrix implementing the modular transformation, we arrive at Cardy's result,

$$g^i_\alpha \, g^i_\beta \, \langle \, i \, | \, i \, \rangle = \sum_j N_{\alpha\beta}{}^j \, S_j{}^i \ . \tag{2.14}$$

These equations can then be solved to find the g^i_α.

One can also show that the same boundary states $|\, \alpha \,\rangle$ describe a circular boundary of radius one in the plane[§] and so the constants Z_α can now be found by expressing the one-point functions on a disc of radius 1 in two different ways as

$${}^{(\alpha)}B^{\mathbb{1}}_i \, Z_\alpha = \langle \, \Phi_i(0) \, \rangle^{\rm disc}_\alpha = \langle \, \alpha \, | \, i \, \rangle = \sum_j g^j_\alpha \, \langle\!\langle \, j \, | \, i \, \rangle = g^i_\alpha \, \langle \, i \, | \, i \, \rangle \ , \tag{2.15}$$

to find

$$Z_\alpha \, {}^{(\alpha)}B^{\mathbb{1}}_i = g^i_\alpha \, \langle \, i \, | \, i \, \rangle \ . \tag{2.16}$$

This completes the identification of the structure constants and zero-point functions. To end this section we recall how to find the conformal values of the g-functions in terms of this conformal data. To fix the g-functions g_α, we note that the leading term in the cylinder partition function is given by

$$Z^{\rm cyl}_{(\alpha\beta)}(R,L) \sim g^\Omega_\alpha \, g^\Omega_\beta \, e^{-RE_\Omega} \, \langle \, \Omega \, | \, \Omega \, \rangle \ . \tag{2.17}$$

where $|\, \Omega \,\rangle$ is the state of lowest conformal weight in the theory defined on the plane. This means that the g-functions g_α satisfy

$$g_\alpha \, g_\beta = g^\Omega_\alpha \, g^\Omega_\beta \, \langle \, \Omega \, | \, \Omega \, \rangle \ . \tag{2.18}$$

However, recalling that the conformal vacuum representation '0' satisfies $N_{0\alpha}{}^i = \delta^i_\alpha$, we see from (2.14) that

$$(g^\Omega_{\mathbb{1}})^2 = \frac{S_{\Omega 0}}{\langle \, \Omega \, | \, \Omega \, \rangle} \ , \quad g^\Omega_{\mathbb{1}} \, g^\Omega_\alpha = \frac{S_{\Omega\alpha}}{\langle \, \Omega \, | \, \Omega \, \rangle} \ . \tag{2.19}$$

Finally, we recall that the modular S-matrix for the Virasoro minimal models satisfies $S_{\Omega\alpha}{>}0$ for all representations α, and so if we require the g-functions to be positive and the g^i_α to be real we should take $\langle \, \Omega \, | \, \Omega \, \rangle > 0$ and can read off their values from eqns. (2.18) and (2.19) as

$$g_{\mathbb{1}} = |S_{\Omega 0}|^{1/2} \ , \quad g_\alpha = \frac{S_{\Omega\alpha}}{|S_{\Omega 0}|^{1/2}} \ , \quad g^\Omega_\alpha = \frac{g_\alpha}{\sqrt{\langle \, \Omega \, | \, \Omega \, \rangle}} \ . \tag{2.20}$$

We now give the explicit results for the case of the Yang-Lee model.

2.1 The Yang-Lee model

The Yang-Lee model is the simplest non-unitary conformal field theory, $M_{2,5}$, and has central charge $-22/5$ and effective central charge $2/5$. There are only two representations of the Virasoro algebra of interest, of weight 0 and $-1/5$, and consequently only two bulk primary

[§] n.b. the normalisations of annulus partition functions differ from those of cylinder partition functions [10], so some care must be taken to define boundary states for discs of general radius.

fields, the identity $\mathbb{1}$ of weight 0, and φ of weight $x_\varphi = -2/5$; equally there are only two conformally-invariant boundary conditions, which we denote by $\mathbb{1}$ and Φ. The fusion rules are

$$\begin{aligned} \mathbb{1} \times \mathbb{1} &= \mathbb{1} \,, \\ \mathbb{1} \times \varphi &= \varphi \,, \\ \varphi \times \varphi &= \mathbb{1} + \varphi \,. \end{aligned} \tag{2.21}$$

From these rules we read off that there are only three non-trivial boundary fields, all of weight $h_\phi = 1/5$. Two of these interpolate the two different conformal boundary conditions,

$$\phi^{(\Phi\mathbb{1})}_{-1/5} \,, \quad \phi^{(\mathbb{1}\Phi)}_{-1/5} \,, \tag{2.22}$$

which we shall both denote by ψ, and one lives on the Φ boundary,

$$\phi \equiv \phi^{(\Phi\Phi)}_{-1/5} \,. \tag{2.23}$$

As indicated[¶], we shall often simply denote the non-trivial boundary primary field on the Φ boundary by ϕ.

If we label the two representations of the Virasoro algebra by ϕ and 1 then the modular S-matrix is

$$S = \begin{pmatrix} S_{11} & S_{1\phi} \\ S_{\phi 1} & S_{\phi\phi} \end{pmatrix} = \tfrac{2}{\sqrt{5}} \begin{pmatrix} -\sin\frac{2\pi}{5} & \sin\frac{\pi}{5} \\ \sin\frac{\pi}{5} & \sin\frac{2\pi}{5} \end{pmatrix} = \begin{pmatrix} -0.8506.. & 0.5257.. \\ 0.5257.. & 0.8506.. \end{pmatrix} \,. \tag{2.24}$$

2.1.1 Yang–Lee structure constants

We give here the structure constants appearing in all the operator products of interest, that is the bulk OPE

$$\varphi(z,\overline{z})\,\varphi(w,\overline{w}) \;=\; C_{\varphi\varphi}{}^{\mathbb{1}}\,|z-w|^{4/5} \;+\; C_{\varphi\varphi}{}^{\varphi}\,|z-w|^{2/5}\,\varphi(w,\overline{w}) \;+\; \dots \,,$$

the boundary OPEs,

$$\begin{aligned} \phi(z)\,\phi(w) &= C_{\phi\phi}{}^{\mathbb{1}}\,|z-w|^{2/5} \;+\; C_{\phi\phi}{}^{\phi}\,|z-w|^{1/5}\,\phi(w) \;+\; \dots \,, \\ \phi(z)\,\psi(w) &= C_{\phi\psi}{}^{\psi}|z-w|^{1/5}\,\psi(w) \;+\; \dots \,, \end{aligned}$$

and the two bulk–boundary OPEs

$$\begin{aligned} \varphi(z)\,|_{\mathbb{1}} &= {}^{(\mathbb{1})}B^{\mathbb{1}}_{\varphi}\,|2(z-w)|^{2/5} \;+\; \dots \,, \\ \varphi(z)\,|_{\Phi} &= {}^{(\Phi)}B^{\mathbb{1}}_{\varphi}\,|2(z-w)|^{2/5} \;+\; {}^{(\Phi)}B^{\phi}_{\varphi}\,|2(z-w)|^{1/5}\,\phi(w) \;+\; \dots \,. \end{aligned}$$

[¶]In this model, there is only a single non-trivial bulk field, a single boundary condition admitting a relevant perturbation, and a single non-trivial boundary field, all labelled by the same Virasoro representation, and hence we have denoted them by φ, Φ and ϕ respectively, in the hope that this will reduce confusion.

We want all these structure constants to be real, and a suitable choice is

$$\begin{aligned} C_{\varphi\varphi}{}^{\mathbb{1}} &= C_{\phi\phi}{}^{\mathbb{1}} = -1\,, \\ C_{\varphi\varphi}{}^{\varphi} &= -\left|\tfrac{2}{1+\sqrt5}\right|^{1/2}\cdot\alpha^2\,, \quad {}^{(\mathbb{1})}B_{\varphi}^{\mathbb{1}} = -\left|\tfrac{2}{1+\sqrt5}\right|^{1/2}\,, \\ C_{\phi\phi}{}^{\phi} &= -\left|\tfrac{1+\sqrt5}{2}\right|^{1/2}\cdot\alpha\,, \quad {}^{(\Phi)}B_{\varphi}^{\mathbb{1}} = \left|\tfrac{1+\sqrt5}{2}\right|^{3/2}\,, \\ C_{\phi\psi}{}^{\psi} &= -\left|\tfrac{2}{1+\sqrt5}\right|^{1/2}\cdot\alpha\,, \quad {}^{(\Phi)}B_{\varphi}^{\phi} = \left|\tfrac{5+\sqrt5}{2}\right|^{1/2}\cdot\alpha\,, \\ \alpha &= \left|\tfrac{\Gamma(1/5)\,\Gamma(6/5)}{\Gamma(3/5)\,\Gamma(4/5)}\right|^{1/2}\,. \end{aligned} \tag{2.25}$$

The state of lowest conformal dimension in the bulk theory is

$$|\,\Omega\,\rangle = |\,\varphi\,\rangle\,, \tag{2.26}$$

and we choose to normalise the bulk highest-weight states as

$$\langle\,0\,|\,0\,\rangle = -1 \quad\Rightarrow\quad \langle\,\varphi\,|\,\varphi\,\rangle = 1\,. \tag{2.27}$$

With this, and demanding $g_\alpha^\varphi > 0$, the coefficients appearing in the boundary states are

$$\begin{aligned} g_{\mathbb{1}}^0 &= \left|\tfrac{\sqrt5+1}{2\sqrt5}\right|^{1/4}\,, \quad g_{\mathbb{1}}^\varphi = \left|\tfrac{\sqrt5-1}{2\sqrt5}\right|^{1/4} \\ g_{\Phi}^0 &= -\left|\tfrac{\sqrt5-2}{\sqrt5}\right|^{1/4}\,, \quad g_{\Phi}^\varphi = \left|\tfrac{2+\sqrt5}{\sqrt5}\right|^{1/4} \end{aligned} \tag{2.28}$$

The zero-point functions are then given as

$$Z_{\mathbb{1}} = \langle\,1\,\rangle_{\mathbb{1}}^{\rm disc} = \langle\,\mathbb{1}\,|\,0\,\rangle = -g_{\mathbb{1}}^0\,, \quad Z_\Phi = \langle\,1\,\rangle_\Phi^{\rm disc} = \langle\,\Phi\,|\,0\,\rangle = -g_\Phi^0\,. \tag{2.29}$$

Finally, the g-functions are given by $g_\alpha = g_\alpha^\Phi\sqrt{\langle\,\varphi\,|\,\varphi\,\rangle} = g_\alpha^\Phi$, i.e.

$$\begin{aligned} \log g_{\mathbb{1}} &= \tfrac14\log\left|\tfrac{\sqrt5-1}{2\sqrt5}\right| = -\tfrac14\log\left|\tfrac{1+\sqrt5}{2}\right| - \tfrac18\log 5 = -0.321482..\,, \\ \log g_{\Phi} &= \tfrac14\log\left|\tfrac{2+\sqrt5}{\sqrt5}\right| = \tfrac34\log\left|\tfrac{1+\sqrt5}{2}\right| - \tfrac18\log 5 = 0.159729..\,. \end{aligned} \tag{2.30}$$

2.1.2 Yang–Lee correlation functions

In terms of the structure constants (2.25), the simple correlation functions (2.5) on a disc of unit radius are

$$\begin{aligned} \langle\ 1\ \rangle_\alpha^{\rm disc} &= Z_\alpha\,, \qquad \langle\ \phi(e^{i\theta})\ \rangle_\Phi^{\rm disc} = 0 \\ \langle\ \varphi(\,re^{i\theta})\ \rangle_\alpha^{\rm disc} &= {}^{(\alpha)}B_\varphi^{\mathbb{1}}\,Z_\alpha\,(1-r^2)^{2/5} \\ \langle\ \phi(e^{i\theta})\,\phi(1)\ \rangle_\Phi^{\rm disc} &= C_{\phi\phi}{}^{\mathbb{1}}\,Z_\Phi\,(2\sin(\theta/2))^{2/5} \\ \langle\ \varphi(\,re^{i\theta}\,)\,\phi(1)\ \rangle_\Phi^{\rm disc} &= {}^{(\Phi)}B_\varphi^{\phi}\,C_{\phi\phi}{}^{\mathbb{1}}\,Z_\Phi\,(1-2r\cos\theta+r^2)^{1/5}(1-r^2)^{1/5} \end{aligned} \tag{2.31}$$

We shall also need two more correlation functions, which are given in terms of chiral four-point blocks. A basis for the chiral four-point functions of the weight $-1/5$ field are f^1 and f^ϕ, given in terms of hypergeometric functions by

$$f^1(x) = [x(1-x)]^{2/5}\,F(\tfrac35,\tfrac45;\tfrac65;x)\,, \quad f^\phi(x) = x^{1/5}\,(1-x)^{2/5}\,F(\tfrac25,\tfrac35;\tfrac45;x)\,. \tag{2.32}$$

In terms of these chiral blocks we can give the bulk two-point functions on a disc of radius 1:

$$\left\langle \varphi(0)\,\varphi(re^{i\theta}) \right\rangle_{\alpha}^{\text{disc}} \;=\; Z_\alpha \left\{ C_{\varphi\varphi}{}^{\mathbb{1}} f^1(r^2) \;+\; {}^{(\alpha)}B_\varphi^{\mathbb{1}}\, C_{\varphi\varphi}{}^{\varphi} f^\phi(r^2) \right\} , \tag{2.33}$$

which is rotationally invariant. We can also give the 1-bulk–2-boundary point functions in terms of these two chiral blocks, but it is more convenient to perform some transformations on the arguments to make the expressions manifestly real, in which case we find

$$\begin{aligned}\left\langle \varphi(0)\;\phi(1)\;\phi(e^{i\theta}) \right\rangle_{\Phi}^{\text{disc}} \;=\; & Z_\Phi\, C_{\phi\phi}{}^{\mathbb{1}} \Big\{ {}^{(\Phi)}B_\varphi^{\mathbb{1}}\, (2\sin\tfrac{\theta}{2})^{2/5}\, (\cos\tfrac{\theta}{2})^{-4/5}\, F(\tfrac{4}{10},\tfrac{9}{10};\tfrac{11}{10};-\tan^2\tfrac{\theta}{2}) \\ & +\; {}^{(\Phi)}B_\varphi^{\phi}\, C_{\phi\phi}{}^{\phi} (2\sin\tfrac{\theta}{2})^{1/5}\, (\cos\tfrac{\theta}{2})^{-3/5}\, F(\tfrac{3}{10},\tfrac{8}{10};\tfrac{9}{10};-\tan^2\tfrac{\theta}{2}) \Big\} .\end{aligned} \tag{2.34}$$

3 g-functions and perturbed conformal field theory

We define the $\mathcal{G}$-functions of the perturbed theory as

$$\mathcal{G}_\alpha = \frac{\langle\, \alpha \,|\, \Omega \,\rangle}{\langle\, \Omega \,|\, \Omega \,\rangle^{1/2}} , \tag{3.1}$$

where $|\,\alpha\,\rangle$ is the (possibly perturbed) boundary state and $|\,\Omega\,\rangle$ is the ground state of the perturbed theory. Typically these functions will not be equal to the g-functions g_α but will differ by the extensive free–energy terms discussed in the introduction:

$$\log \mathcal{G}_\alpha = \log g_\alpha \;-\; L\, f_\alpha^{\text{pcft}} .$$

However it is the $\mathcal{G}_\alpha$ that are accessible in conformal perturbation theory, and not the g_α. Currently it is not possible to determine f_α^{pcft} directly from conformal perturbation theory, but using the truncated conformal space approximation (TCSA), it is possible to approximate the functions $\mathcal{G}_\alpha$ numerically for a reasonable range of L, and this will enable us in some cases to estimate f_α^{pcft}. For the case of the Yang–Lee model, the boundary conditions of interest are $\mathbb{1}$ (which admits no relevant perturbation) and $\Phi(h)$, the perturbation of the conformal Φ boundary by the integral along the boundary

$$h \int \phi(x)\, \mathrm{d}x . \tag{3.2}$$

The bulk perturbation corresponds to a term in the action

$$\lambda \int \varphi(w,\overline{w})\, \mathrm{d}^2 w . \tag{3.3}$$

The functions $\mathcal{G}_\alpha$ therefore have expansions

$$\begin{aligned}\log \mathcal{G}_{\mathbb{1}}(\lambda, L) &= \textstyle\sum_{n=0}^{\infty} d_n\, (\lambda L^{12/5})^n , \\ \log \mathcal{G}_{\Phi(h)}(\lambda, L) &= \textstyle\sum_{m,n=0}^{\infty} c_{mn}\, (hL^{6/5})^m (\lambda L^{12/5})^n .\end{aligned} \tag{3.4}$$

In section 3.3 we discuss the TCSA calculation of $\mathcal{G}_\alpha$, but before that, in the next section we calculate the following coefficients in their expansions:

$$\begin{aligned} \log \mathcal{G}_{\mathbb{1}}(\lambda, L) &= \log g_{\mathbb{1}} \;+\; d_1\,(\lambda L^{12/5}) \;+\; \dots\;, \\ \log \mathcal{G}_{\Phi(h)}(\lambda, L) &= \log g_{\Phi} \;+\; c_{10}\,(hL^{6/5}) \;+\; c_{20}\,(hL^{6/5})^2 \;+\; c_{01}\,(\lambda L^{12/5}) \;+\; \dots \end{aligned} \tag{3.5}$$

To the order to which we will work, the bulk and boundary perturbations can be treated independently, so we shall first calculate c_{01} and d_1, and then c_{10} and c_{20}.

3.1 The bulk perturbation

For a purely bulk perturbation (3.3), after mapping to the plane, the Hamiltonian of the perturbed theory is

$$\begin{aligned} \widehat{H}^{\rm circ}(\lambda, L) &= \widehat{H}_0 \;+\; \lambda\,\widehat{H}_1 \\ &= \frac{2\pi}{L}(L_0 + \overline{L}_0 - \frac{c}{12}) \;+\; \lambda\,\left(\frac{L}{2\pi}\right)^{7/5} \oint \varphi(e^{i\theta})\,\mathrm{d}\theta\;. \end{aligned} \tag{3.6}$$

The full ground state is given by

$$|\,\Omega\,\rangle = |\,\varphi\,\rangle + \lambda \sum_a{}' \Omega_a |\,\psi_a\,\rangle + O(\lambda^2)\;, \tag{3.7}$$

where the sum is over an orthonormal eigenbasis of $\widehat{H}_0$ (where the $'$ indicates that the ground state $|\,\varphi\,\rangle$ is to be excluded) and the coefficients Ω_a are given by first order perturbation theory as

$$\Omega_a = \frac{\langle\,\psi_a\,|\,\widehat{H}_1\,|\,\varphi\,\rangle}{\langle\,\varphi\,|\widehat{H}_0|\,\varphi\,\rangle - \langle\,\psi_a\,|\widehat{H}_0|\,\psi_a\,\rangle}\;. \tag{3.8}$$

Combining (3.8) and (3.6), we find

$$\sum_a{}' \Omega_a |\,\psi_a\,\rangle = -\left(\frac{L}{2\pi}\right)^{12/5} (1-P)\,\frac{1}{L_0 + \overline{L}_0 + 2/5}\,(1-P) \oint \varphi(e^{i\theta})\,|\,\varphi\,\rangle\,\mathrm{d}\theta\;, \tag{3.9}$$

where $P = |\,\varphi\,\rangle\langle\,\varphi\,|$ is the projector onto the state $|\,\varphi\,\rangle$. From (3.7), the norm of $|\,\Omega\,\rangle$ is unchanged to order λ, and hence the correction to the $\mathcal{G}$-function is given by

$$\log \frac{\mathcal{G}_\alpha(\lambda, L)}{\mathcal{G}_\alpha(0, L)} = \lambda L^{12/5} a_\alpha + O(\lambda^2)\;, \tag{3.10}$$

where

$$a_\alpha = -\frac{1}{g_\alpha}(2\pi)^{-12/5} \oint \mathrm{d}\theta \langle\,\alpha\,|(1-P)\frac{1}{L_0 + \overline{L}_0 + 2/5}(1-P)\,\varphi(e^{i\theta})\,|\,\varphi\,\rangle\;. \tag{3.11}$$

Using the rotational invariance of the boundary state and of $\langle\,\varphi\,|$ and the relations

$$\int_0^1 x^\alpha\,\mathrm{d}x = \frac{1}{\alpha+1}\;,\quad x^{L_0+\overline{L}_0}\,\varphi(1)\,x^{-L_0-\overline{L}_0} = x^{-2/5}\,\varphi(x)\;,\quad \langle\,\alpha\,|P = g_\Phi \langle\,\varphi\,|\;,$$

we arrive at

$$a_\alpha = -(2\pi)^{-7/5} \int_0^1 \frac{\mathrm{d}x}{x^{7/5}} \left(\frac{1}{g_\alpha} \langle\, \alpha \,|\varphi(x)|\, \varphi \,\rangle \;-\; \langle\, \varphi \,|\varphi(x)|\, \varphi \,\rangle \right) . \tag{3.12}$$

The correlation functions in (3.12) are

$$\begin{aligned} \langle\, \alpha \,|\, \varphi(x) \,|\, \varphi \,\rangle &= \langle\, \varphi(x)\varphi(0) \,\rangle_\alpha^{\mathrm{disc}} \;=\; Z_\alpha \left\{ C_{\varphi\varphi}{}^{\mathbb{1}} f^1(x^2) \;+\; {}^{(\alpha)}B_\varphi^{\mathbb{1}}\, C_{\varphi\varphi}{}^{\varphi} f^\phi(x^2) \right\} \\ \langle\, \varphi \,|\, \varphi(x) \,|\, \varphi \,\rangle &= -C_{\varphi\varphi}{}^{\varphi}\, x^{2/5} , \end{aligned}$$

so that using (2.16), the expression for a_α simplifies to

$$a_\alpha = -(2\pi)^{-7/5} \Big(C_{\varphi\varphi}{}^{\varphi}\, I_2 \;+\; \frac{C_{\varphi\varphi}{}^{\mathbb{1}}}{{}^{(\alpha)}B_\varphi^{\mathbb{1}}}\, I_1 \Big) , \tag{3.13}$$

where the integrals I_1 and I_2 are given (by Mathematica) as

$$\begin{aligned} I_1 &= \int_0^1 \frac{\mathrm{d}x}{x^{7/5}} f^1(x^2) \;=\; \int_0^1 \mathrm{d}x\; x^{-3/5} (1-x^2)^{2/5} F(\tfrac{3}{5}, \tfrac{4}{5}; \tfrac{6}{5}; x^2) \\ &= \frac{\pi}{10 \sin(2\pi/5)} \frac{\Gamma(\frac{1}{5})\,\Gamma(\frac{2}{5})}{\Gamma(\frac{4}{5})^2} \;=\; 2.48171... , \end{aligned}$$

and the somewhat obscure expression

$$\begin{aligned} I_2 &= \int_0^1 \frac{\mathrm{d}x}{x^{7/5}} (f^\phi(x^2) - x^{2/5}) \;=\; \int_0^1 \frac{\mathrm{d}x}{x} \Big((1-x^2)^{2/5} F(\tfrac{2}{5}, \tfrac{3}{5}; \tfrac{4}{5}; x^2) - 1 \Big) \\ &= -\tfrac{15}{56}\, {}_3F_2(1, \tfrac{7}{5}, \tfrac{8}{5}; \tfrac{9}{5}, \tfrac{12}{5}; 1) + \tfrac{\pi}{8}\, \tfrac{(5+\sqrt{5})^{3/2}}{\sqrt{10}} - \tfrac{\sqrt{5}}{4} \log \tfrac{1+\sqrt{5}}{2} + \tfrac{5}{8}(\log 5 - 2) \\ &= -0.083937990... . \end{aligned} \tag{3.14}$$

Substituting these values into a_α we find

$$d_1 \;=\; a_{\mathbb{1}} \;=\; -(2\pi)^{-7/5} \Big(C_{\varphi\varphi}{}^{\varphi}\, I_2 \;+\; \frac{C_{\varphi\varphi}{}^{\mathbb{1}}}{{}^{(\mathbb{1})}B_\varphi^{\mathbb{1}}}\, I_1 \Big) \;=\; -0.25311758.. , \tag{3.15}$$

$$c_{01} \;=\; a_\Phi \;=\; -(2\pi)^{-7/5} \Big(C_{\varphi\varphi}{}^{\varphi}\, I_2 \;+\; \frac{C_{\varphi\varphi}{}^{\mathbb{1}}}{{}^{(\Phi)}B_\varphi^{\mathbb{1}}}\, I_1 \Big) \;=\; 0.0797648257.. . \tag{3.16}$$

While the expression for I_2 is rather unwieldy, it cancels exactly from the ratio

$$\log \frac{\mathcal{G}_\Phi(\lambda, L)}{\mathcal{G}_{\mathbb{1}}(\lambda, L)} \;=\; \log \frac{g_\Phi}{g_{\mathbb{1}}} - (\lambda L^{12/5})(2\pi)^{-7/5} I_1 C_{\varphi\varphi}{}^{\mathbb{1}} \left(\tfrac{1}{{}^{(\Phi)}B_\varphi^{\mathbb{1}}} - \tfrac{1}{{}^{(\mathbb{1})}B_\varphi^{\mathbb{1}}} \right) + \ldots , \tag{3.17}$$

so that CPT predicts

$$c_{01} - d_1 = (2\pi)^{-2/5}\, 5^{-3/4}\, \frac{\Gamma(\frac{1}{5})\,\Gamma(\frac{2}{5})}{(1+\sqrt{5})\,\Gamma(\frac{4}{5})^2} = 0.3328824.. . \tag{3.18}$$

In section 5 we shall compare this with the TBA results from section 4.

3.2 The boundary perturbation

The boundary condition $\Phi(h)$ corresponds to the perturbation of the Φ boundary by the addition to the action of the term

$$\delta S = h \int |\mathrm{d}z|\, \phi(z) \ . \tag{3.19}$$

To calculate c_{10} and c_{20} we can assume that the bulk theory is unperturbed which means that we can replace the ground state $|\,\Omega\,\rangle$ by $|\,\varphi\,\rangle$. The perturbed boundary state is

$$\langle\, \Phi(h)\,| = \langle\, \Phi\,| \Big(1 - \delta S + \tfrac{1}{2}(\delta S)^2 + \ldots \Big) \ ,$$

and so the coefficients in the expansion

$$\langle\, \Phi(h)\,|\,\varphi\,\rangle = g_\Phi \left(1 \ + \ \widetilde{c}_{10}\, hL^{6/5} \ + \ \widetilde{c}_{20}\, (hL^{6/5})^2 \ + \ \ldots \right) \tag{3.20}$$

can be written in terms of the simple disc amplitudes

$$\begin{aligned} \widetilde{c}_{10} &= -\frac{(2\pi)^{-6/5}}{g_\Phi} \int_0^{2\pi} \Big\langle\ \phi(e^{i\theta})\ \varphi(0)\ \Big\rangle_\Phi^{\mathrm{disc}}\ \mathrm{d}\theta \ , \\ \widetilde{c}_{20} &= \tfrac{1}{2}\frac{(2\pi)^{-12/5}}{g_\Phi} \int_0^{2\pi}\int_0^{2\pi} \Big\langle\ \phi(e^{i\theta})\ \phi(e^{i\theta'})\ \varphi(0)\ \Big\rangle_\Phi^{\mathrm{disc}}\ \mathrm{d}\theta\, \mathrm{d}\theta' \ . \end{aligned} \tag{3.21}$$

The correlation functions appearing in (3.21) are given in section 2.1.2. The two-point function $\langle\, \varphi(0)\phi(e^{i\theta})\,\rangle_\Phi^{\mathrm{disc}}$ is rotationally invariant and so the integration in $\widetilde{c}_{10}$ is trivial, giving

$$\widetilde{c}_{10} = -(2\pi)^{-1/5} \frac{{}^{(\Phi)}B_\varphi^\phi C_{\phi\phi}{}^{\mathbb{1}}}{{}^{(\Phi)}B_\varphi^{\mathbb{1}}} = (2\pi)^{-1/5} 5^{1/4} \left| \frac{\Gamma(\frac{2}{5})\Gamma(\frac{6}{5})}{2\cos(\pi/5)\Gamma(\frac{4}{5})^2} \right|^{1/2} = 0.99777.. \tag{3.22}$$

It is a little more complicated to find $\widetilde{c}_{20}$, which is given as

$$\widetilde{c}_{20} = (2\pi)^{-7/5} \left\{ C_{\phi\phi}{}^{\mathbb{1}}\, I_3 \ + \ C_{\phi\phi}{}^{\phi}\, C_{\phi\phi}{}^{\mathbb{1}}\, \frac{{}^{(\Phi)}B_\varphi^\phi}{{}^{(\Phi)}B_\varphi^{\mathbb{1}}}\, I_4 \right\} \ , \tag{3.23}$$

where the integrals I_3 and I_4 are given by

$$\begin{aligned} I_3 &= \int_0^\pi (2\sin\tfrac{\theta}{2})^{2/5} (\cos\tfrac{\theta}{2})^{-4/5} F(\tfrac{4}{10}, \tfrac{9}{10}; \tfrac{11}{10}; -\tan^2\tfrac{\theta}{2})\ \mathrm{d}\theta \ , \\ I_4 &= \int_0^\pi (2\sin\tfrac{\theta}{2})^{1/5} (\cos\tfrac{\theta}{2})^{-3/5} F(\tfrac{3}{10}, \tfrac{8}{10}; \tfrac{9}{10}; -\tan^2\tfrac{\theta}{2})\ \mathrm{d}\theta \ , \end{aligned} \tag{3.24}$$

which do not seem to have simple closed expressions. However, by making use of the substitution $v = \cos^2(\theta/2)$ and the explicit forms for the structure constants appearing in (3.23), one can show that the specific combination of I_3 and I_4 in (3.23) is given by

$$\widetilde{c}_{20} = \frac{1}{\sqrt{5}}\, (\widetilde{c}_{10})^2 \ . \tag{3.25}$$

Taking the logarithm of (3.20), we find

$$\log \mathcal{G}_{\Phi(h)}(0,L) = \log g_\Phi \ + \ \widetilde{c}_{10} h L^{6/5} \ + \ (\widetilde{c}_{20} - \tfrac{1}{2}(\widetilde{c}_{10})^2)\,(hL^{6/5})^2 \ + \ \dots \ , \tag{3.26}$$

so that the coefficients c_{10} and c_{20} in (3.5) are given by

$$\begin{aligned} c_{10} &= (2\pi)^{-1/5} 5^{1/4} \left| \frac{\Gamma(\frac{2}{5})\Gamma(\frac{6}{5})}{2\cos(\pi/5)\Gamma(\frac{4}{5})^2} \right|^{1/2} = 0.99777.. \ , \\ c_{20} &= \left(\tfrac{1}{\sqrt{5}} - \tfrac{1}{2}\right) (c_{10})^2 \ . \end{aligned} \tag{3.27}$$

The coefficients c_{10} and c_{20} have also been calculated using the free-field construction in [22], with the same results that we find.

3.3 Evaluating $\log(g_\alpha)$ using the TCSA method

The truncated conformal space approximation (TCSA) introduced in [11] gives numerical approximations to the lowest eigenvalues of the Hamiltonian of a perturbed conformal field theory by restricting the Hamiltonian to a finite dimensional subspace, working out the matrix elements exactly and diagonalising the resulting matrix numerically.

Originally developed for systems on a circle, we outlined in [4] how this method can also be applied to a system on a strip with conformal boundary conditions α, β on the two ends and perturbed simultaneously by a bulk field Φ of weight x_Φ and by boundary fields ϕ_l and ϕ_r of weights x_l and x_r. The resulting Hamiltonian is

$$\begin{aligned} &\widehat{H}(R,\lambda,h_l,h_r) \\ &= \frac{\pi}{R}\Big(L_0 - \tfrac{c}{24} \ + \ \lambda \left|\tfrac{R}{\pi}\right|^{2-x_\Phi} \int_{\theta=0}^{\pi} \Phi(\exp(i\theta))\,\mathrm{d}\theta \ + \ h_l \left|\tfrac{R}{\pi}\right|^{1-x_l} \phi_l(-1) \ + \ h_r \left|\tfrac{R}{\pi}\right|^{1-x_r} \phi_r(1) \Big) \ . \end{aligned}$$

The matrix elements of $\widehat{H}$ can be easily calculated numerically and the Hamiltonian diagonalised on spaces of the order of 100 states.

The partition function on a cylinder of circumference L can be estimated numerically as the trace over the finite-dimensional truncated space.

$$Z_{\alpha(h_l)\beta(h_r)}(L,R,\lambda) = \mathrm{Tr}(\exp(-L\widehat{H}(R,\lambda,h_l,h_r))) \ .$$

More details will be given in the next section where the method is applied to perturbations of the $\mathbb{1}$ and $\Phi(0)$ boundary conditions, both by bulk perturbations, and (for the $\Phi(0)$ boundary condition) at the boundary. In the presence of the bulk perturbation, the mass scale is set by the mass M of the single massive particle of the scaling Yang–Lee model, which is related to λ by [12, 13]

$$M = \kappa \lambda^{5/12} \ , \quad \kappa = 2^{19/12}\sqrt{\pi}\,\frac{\left(\Gamma(3/5)\Gamma(4/5)\right)^{5/12}}{5^{5/16}\Gamma(2/3)\Gamma(5/6)} = 2.642944\dots \ ,$$

We present the results for the $(\mathbb{1},\mathbb{1})$ and $(\mathbb{1},\Phi(h))$ boundary conditions in the next two sections.

3.3.1 The strip with $(\mathbb{1},\mathbb{1})$ boundary conditions

The $(\mathbb{1},\mathbb{1})$ system has no relevant boundary perturbations and so the strip Hamiltonian is simply

$$\widehat{H}(R,\lambda) = \frac{\pi}{R}\Big(L_0 - \tfrac{c}{24} \;\; + \;\; \lambda\,|\tfrac{R}{\pi}|^{2-x_\Phi} \int_{\theta=0}^{\pi} \Phi(\exp(i\theta))\,\mathrm{d}\theta\Big)\ .$$

The spectrum comprises scattering states of a single massive particle of mass M and no boundary bound states. In figure 1 we plot the 15 lowest eigenvalues of $\widehat{H}/M$ against $r = MR$ (as estimated from TCSA with 29 states).

We estimate the partition function by taking the sum over all the TCSA eigenvalues E_i^{TCSA} at the given truncation level

$$Z(r,l) = \sum_i \exp(-LE_i^{\mathrm{TCSA}})\ ,$$

where $l = ML$. For any particular l, we expect that the behaviour of $Z(r,l)$ for small r is dominated by the conformal point, while at large r truncation errors will dominate. If we are lucky, there will be an intermediate range of r (the scaling region) in which $Z(r,l)$ exhibits the scaling form

$$\log Z(r,l) \sim -a(l)\,r + b(l) + \dots\ . \tag{3.28}$$

From equations (1.1), (1.3) and (3.1), we expect that

$$a(l) = \frac{E_0^{\mathrm{cyl}}}{M}\ , \quad b(l) = 2\log \mathcal{G}_{\mathbb{1}}(l)\ .$$

To test for the behaviour (3.28) we plot $\log(\mathrm{d}\log Z(r,l)/\mathrm{d}r)$ to see if, for given l, there is a region in r for which it is approximately constant. In figure 2 we plot $\log(\mathrm{d}\log Z(r,l)/\mathrm{d}r)$ against $\log(r/l)$ for various fixed values of l calculated using the TCSA with 19 states and with 106 states. For small values of l we see the typical behaviour expected – as r increases, $\log(\mathrm{d}\log Z(r,l)/\mathrm{d}r)$ flattens out to a scaling region in which it is approximately constant before truncation effects take over. We can be fairly sure that this is indeed the scaling region by comparing the behaviour for different truncation levels, and, as expected, increasing the truncation level extends the scaling region further into the IR. On close examination we find for small $l \lesssim 1$ that the scaling region is centred on $\log(r/l) \sim 1.21$ for 19 states and on $\log(r/l) \sim 1.46$ for 106 states. Hence we shall take the TCSA estimates of $a(l)$ and $b(l)$ to be those at $\log(r/l) = 1.21$ and $\log(r/l) = 1.46$ for 19 and 106 states respectively. For larger values of $l > 1$ the effects of truncation start to interfere for $\log r \sim 2.75$ and it is not clear whether we have actually reached the scaling region or not.

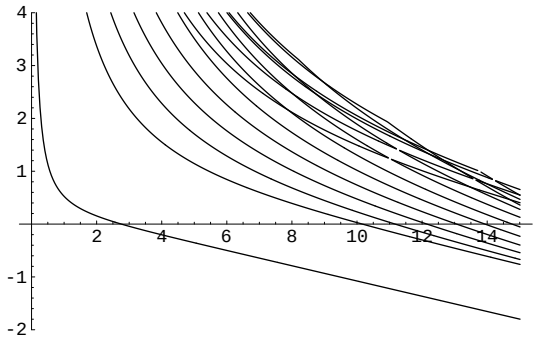

Figure 1: The first 15 eigenvalues of $\widehat{H}/M$ for the $(\mathbb{1},\mathbb{1})$ system plotted against r from TCSA with 29 states.

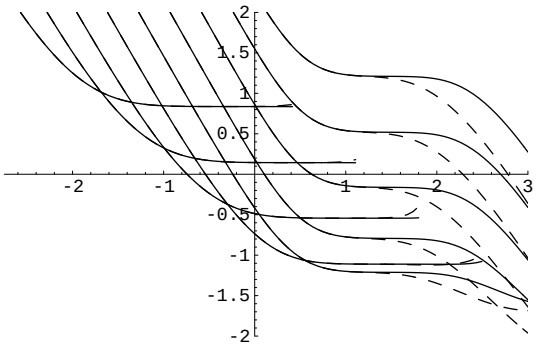

Figure 2: Plots of $\log(\mathrm{d}\log Z(r,l)/\mathrm{d}r)$ vs. $\log(r/l)$ for $l{=}2^n$, with (from left to right) $n = 4,3,2,1,0,-1,-2,-3,-4$. Results are for 106 (solid) and for 19 (dashed) states.

In figure 3 we plot $a(l)$ as estimated in this way from the TCSA with 106 states and include a plot of $E_0^{\mathrm{circ}}(l)/M$ for comparison. It is clear from the graph that it is possible to estimate $a(l)$ effectively this way.

In figure 4 we plot $b(l)$ as estimated in the same way. The onset of the linear behaviour (1.4) expected for large l is clear in this plot. In figure 5 we plot $\mathrm{d}b(l)/\mathrm{d}l$ and give for comparison the exact TBA prediction from eqn. (4.20). It is clear that while the TCSA cannot predict the correct value, it agrees with the TBA to our accuracy, and so in figure 6 we plot the combination

$$Lf_{\mathbb{1}}^{\mathrm{TBA}} + \log \mathcal{G}_{\mathbb{1}}^{\mathrm{TCSA}}(l)\ , \quad f_{\mathbb{1}}^{\mathrm{TBA}} = \tfrac{1}{4}(\sqrt{3}-1)\ ,$$

showing its interpolation between the UV and IR values. Finally in table 1 we give the TCSA estimate of the coefficients $\mathcal{G}^{(n)}(0)/n!$ of the series expansion (3.4) from truncations to finite dimensional spaces and the extrapolation of these coefficients to infinite level:

	TCSA					
	63 states	75 states	90 states	106 states	∞ states	exact
d_0	-0.321615	-0.321558	-0.321518	-0.321580	-0.3215	$-0.32148269..$
d_1	-0.25230	-0.25252	-0.25269	-0.25260	-0.253	$-0.25311758..$
d_2	0.076715	0.077208	0.077523	0.077570	0.0775	—
d_3	-0.03510	-0.03569	-0.03599	-0.03606	-0.0360	—
d_4	0.01787	0.01841	0.01857	0.01893	0.019	—

Table 1

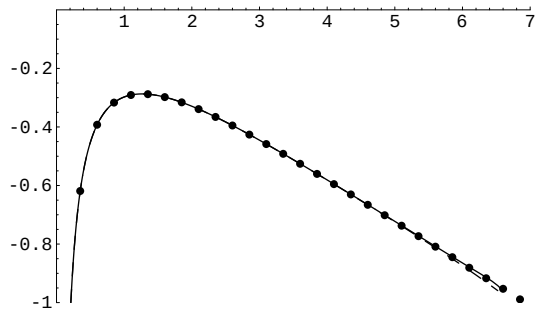

Figure 3: $a(l)$ as estimated from TCSA with 19 states (dashed line) and 106 states (solid line) together with $E_0^{\rm circ}(l)/M$ (points) plotted against l.

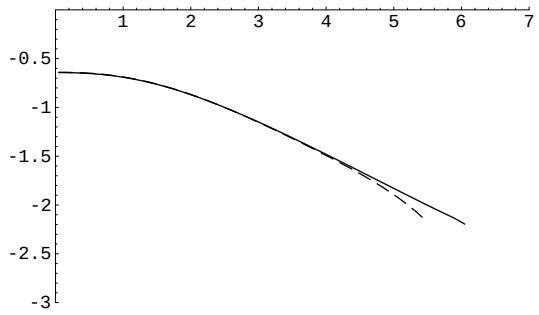

Figure 4: $b(l)$ as estimated from TCSA with 19 states (dashed line) and 106 states (solid line) plotted against l.

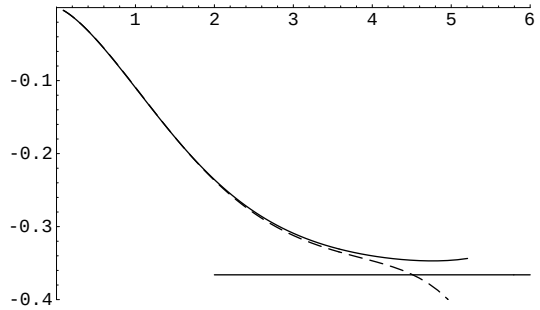

Figure 5: $\mathrm{d}b/\mathrm{d}l$ as estimated from TCSA with 19 states (dashed line) and 106 states (solid line) plotted against l. Also shown is the TBA prediction $-2f_{\mathbb{1}}^{TBA}$.

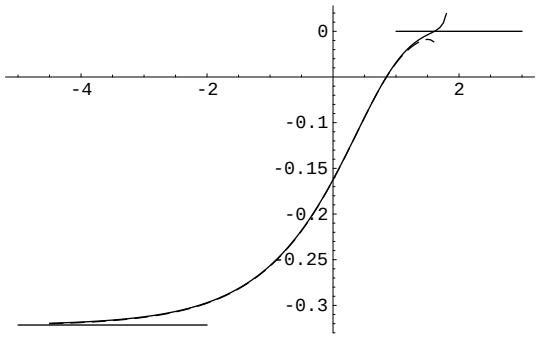

Figure 6: $\log g_{\mathbb{1}}(l)$ vs. $\log l$ from $f_{\mathbb{1}}^{\rm TBA}$ and the $\mathcal{G}$-function from the TCSA with 19 (dashed line) and 106 (solid line) states. Also shown are the exact UV and IR values.

3.3.2 The strip with $(\mathbb{1}, \Phi(h))$ boundary conditions: massive case

We now consider the strip with boundary conditions $(\mathbb{1}, \Phi(h))$, corresponding to a Hamiltonian

$$\widehat{H}(R,\lambda,h) = \frac{\pi}{R}\Big(L_0 - \tfrac{c}{24} \;+\; \lambda\,\big|\tfrac{R}{\pi}\big|^{12/5}\int_{\theta=0}^{\pi}\varphi(\exp(i\theta))\,\mathrm{d}\theta \;+\; h\,\big|\tfrac{R}{\pi}\big|^{6/5}\,\phi(1)\Big)\,. \tag{3.29}$$

The general partition function is now a function of three dimensionless combinations of R, L, λ and h. In the massive case it is convenient to take these as the scaled lengths and the scaled boundary field, defined by

$$r = M\,R\,, \quad l = M\,L\,, \quad \widehat{h} = h\,M^{-6/5}\,, \tag{3.30}$$

with the expectation that

$$\log Z_{(\mathbb{1},\Phi(h))}(R,L,\lambda) \;\sim\; -r\,a(l,\widehat{h}) \;+\; b(l,\widehat{h})\,, \tag{3.31}$$

$$b(l,\widehat{h}) = \log(\,\mathcal{G}_{\mathbb{1}}(L,\lambda)\,\mathcal{G}_{\Phi(h)}(L,\lambda)\,) \;\sim\; -\frac{l}{M}\,(f_{\Phi(\widehat{h})} + f_{\mathbb{1}}) \;+\; \log(\,g_{\mathbb{1}}(l)\,g_{\Phi(\widehat{h})}(l)\,)\,. \tag{3.32}$$

To simplify matters, in this section we will only discuss the model with a purely bulk perturbation, so that $h = 0$. This corresponds to the value $b = -1/2$ of the IR boundary parameter defined in eqn. (4.4). In figure 7 we show the spectrum of the model with these boundary conditions and truncation to 81 states (the first excited state here is actually a boundary bound state). Examining $\mathrm{d}\log(Z(r,l))/\mathrm{d}r$, we find that, as before, for small values of l there is a scaling region in r which broadens with increasing l before truncation effects intervene. For 140 states, the small l scaling region is centred on $\log(r/l) \sim 1.38$ while for large l truncation effects occur for $\log r \sim 1.5$. For small l we can clearly see that scaling has set in and can be confident that we can estimate $a(l)$ and $b(l)$ using the values at the midpoint of the scaling region. For large l we can assume that the 'best guesses' of $a(l)$ and $b(l)$ are given by their values at either (a) the small l effective value of r, or (b) the largest value of r before truncation effects are obvious. In other words we consider the two estimates of $r_{\mathrm{eff}}(l)$ defined by

$$(a)\ \log r_{\mathrm{eff}}(l) = 1.38 + \log l\ , \qquad \text{and } (b)\ \log r_{\mathrm{eff}}(l) = \min(\ 1.38 + \log l\ ,\ 1.5\ )\ .$$

In figures 8 and 9 we plot $a(l)$ and $\mathrm{d}b/\mathrm{d}l$ using these two methods. We see that this second method of taking the 'best guess' at the large l values gives quite pleasing results for these two quantities while having the problem that the errors are hard to estimate. In figure 10 we plot $\log(g_{\mathbb{1}}(l)\, g_{\Phi(0)}(l))$ using method (b) and compare the results using the TBA value of f_α and a 'fitted value' as was used in [4]. As we see, the large l behaviour of the g-function appears to be improved by using a 'fitted' value of f_α, but again the errors induced by doing this are unknown.

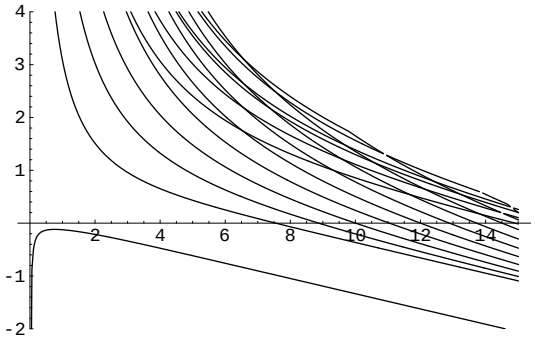

Figure 7: The first 15 eigenvalues of $\widehat{H}/m$ for the $(\mathbb{1}, \Phi(0))$ system plotted against r from TCSA with 81 states.

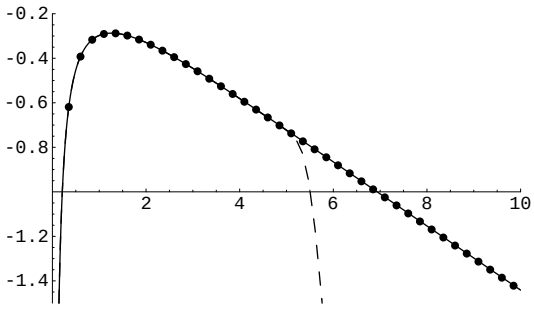

Figure 8: $a(l)$ vs. l, as estimated from TCSA with 140 states using methods (a) (dashed line) and (b) (solid line), together with $E_0^{\mathrm{circ}}(l)/M$ (points).

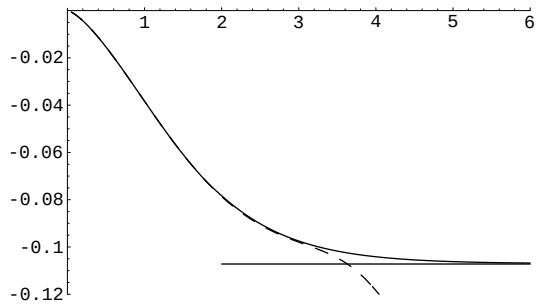

Figure 9: $\mathrm{d}b/\mathrm{d}l$ as estimated from TCSA with with 140 states using methods (a) (dashed line) and (b) (solid line), together with the TBA prediction.

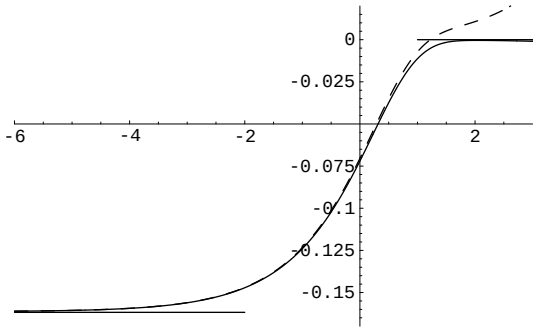

Figure 10: $\log(g_{\mathbb{1}}(l)\, g_{\Phi(0)}(l))$ vs. $\log l$ from the TCSA with 140 states using method (b) and f_α^{TBA} (dashed line) and a fitted value of f_α (solid line). Also shown are the exact UV and IR values.

In table 2 we give the coefficients in the power series expansion (3.4) as found from the TCSA data by estimating the n-th derivatives of $\log(\mathcal{G}_{\mathbb{1}}\mathcal{G}_{\Phi(0)})$ wrt λ at $\lambda = 0$. We also give the result of extrapolating these coefficients to infinite level.

Combined with the results for d_m in table 1 we can then estimate the coefficients $(c_{0m} - d_m)$ which appear in the expansion of the ratio $\log(\mathcal{G}_{\Phi(h)}/\mathcal{G}_{\mathbb{1}})$. These are compared with the results from the TBA in section 5, table 7.

	TCSA					exact
	81 states	98 states	117 states	140 states	∞ states	
$c_{00} + d_0$	-0.16089	-0.16108	-0.16123	-0.1613	-0.162	$-0.161753565..$
$c_{01} + d_1$	-0.1754	-0.1750	-0.1748	-0.1746	-0.174	$-0.173352755..$
$c_{02} + d_2$	0.06745	0.06703	0.06712	0.06676	0.0628	—
$c_{03} + d_3$	-0.0370	-0.0370	-0.0366	-0.0363	-0.033	—
$c_{04} + d_4$	0.02248	0.02267	0.02230	0.02225	0.02	—

Table 2: The coefficients $(c_{0n}+d_n)$ from TCSA and CPT

3.3.3 $(\mathbb{1}, \Phi(h))$ boundary conditions: massless case

We now consider the $(\mathbb{1}, \Phi(h))$ model with the bulk massless. For this case, the three combinations (3.30) do not make much sense, and it is better to consider the system as a function of the two variables

$$\widetilde{r} = r/l = R/L\,, \quad \widetilde{h} = \widehat{h}\, l^{6/5} = h\, L^{6/5}\,. \tag{3.33}$$

As was shown in figure 1(b) of our previous paper [4], the spectrum of $\widehat{H}$ here is real for $\widetilde{h}$ positive, and for $\widetilde{h} \gg 1$ approaches that of the strip with $(\mathbb{1}, \mathbb{1})$ boundary conditions. For sufficiently negative $\widetilde{h}$, the spectrum becomes complex.

The Hamiltonian on the circle is unperturbed if the bulk is massless, and so the ground state energy on the circle is simply given by (2.10):

$$R\, E_0^{\mathrm{circ}}(0) = -\frac{\pi}{15}\,\frac{R}{L} = -\frac{\pi}{15}\,\widetilde{r}\,.$$

Similarly the massless limit of the linear term in $\mathcal{G}$, (Lf_b), is simply given by (4.21), so that (3.31) and (3.32) become

$$\log Z_{(\mathbb{1},\Phi(h))}(R,L,0) \;\sim\; \frac{\pi}{15}\,\widetilde{r} \;+\; b(\widetilde{h})\;, \tag{3.34}$$

$$b(\widetilde{h}) \;\sim\; -2^{-1/6}\left|\frac{\widetilde{h}}{h_c}\right|^{5/6} + \log(g_{\Phi(h)}(L,0))\;. \tag{3.35}$$

In figures 11a–11c we show the TCSA estimates of $Z(\widetilde{r},\widetilde{h})$ for various values of $\widetilde{h}$ for truncations to 29, 67 and 140 states. There is good convergence for $\widetilde{r} \lesssim 8$.

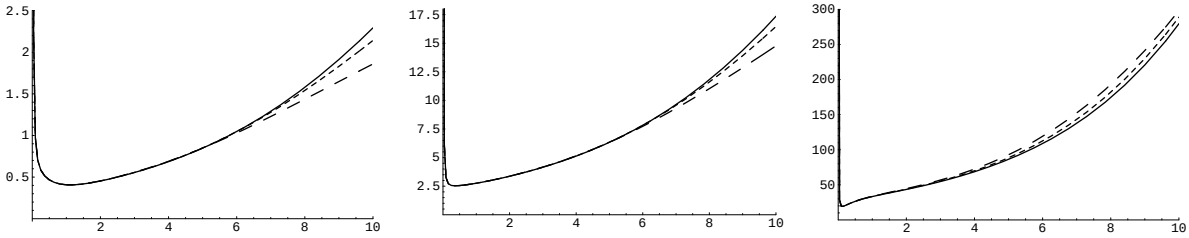

(a) $\widetilde{h} = -1\;.$ (b) $\widetilde{h} = 1\;.$ (c) $\widetilde{h} = 4\;.$

Figure 11: Graphs of $\log Z$ vs. $\widetilde{r}$ for fixed values of $\widetilde{h}$ from the TCSA to 29 states (dashed line), 67 states (dotted line) and 140 states (solid line)

In figures 12a–12c we plot $\log(\mathrm{d}\log(Z(\widetilde{r},\widetilde{h}))/\mathrm{d}\widetilde{r})$ vs. $\widetilde{r}$ to show the scaling region in which $\log Z$ grows approximately linearly, and include the exact value $\log(\pi/15)$ from eqn. (3.34) for comparison. We see from these graphs that for small values of $\widetilde{h}$ there is good convergence for $\widetilde{r} \lesssim 3-6$.

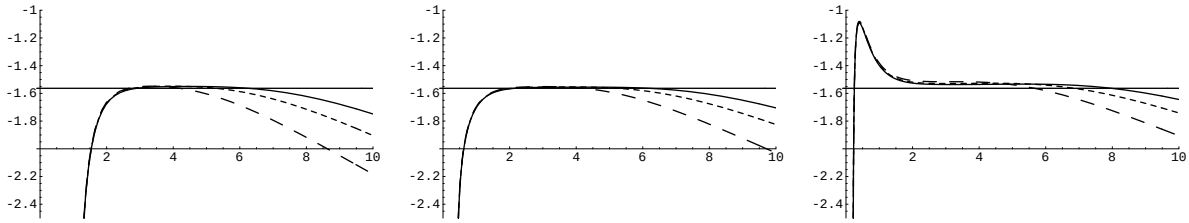

(a) $\widetilde{h} = -1\;.$ (b) $\widetilde{h} = 1\;.$ (c) $\widetilde{h} = 2\;.$

Figure 12: Graphs of $\log(\mathrm{d}\log Z/\mathrm{d}\widetilde{r})$ vs. $\widetilde{r}$ for fixed values of $\widetilde{h}$ from the TCSA to 29 states (dashed line), 67 states (dotted line) and 140 states (solid line). Also shown is the exact value $\log(\pi/15)$.

We can estimate $b(\widetilde{h})$ in two ways – using the exact value of RE_0^{circ} or using the TCSA value calculated using eqn. (3.32). With $b(\widetilde{h})$ calculated in either manner we can finally use the TBA value of (fL) to calculate the g-function from eqn. (3.35). In figure 13 we plot the TCSA estimate of $\log(g_\Phi(h))$ using the exact value of E_0^{circ} and the estimated value, together with

the massless TBA result (suitably normalised). We see that there is excellent agreement.

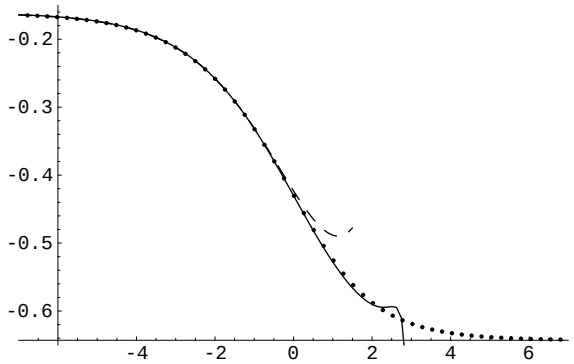

Figure 13: Graphs of $\log(g_\Phi(\widetilde{h}))$ vs. $\log(\widetilde{h})$ from the TCSA with 140 states using the exact value of $E_0^{\rm circ}$ (dashed line) and the estimated value (solid line) together with the TBA results (points).

As a further check, in table 3 we give the TCSA estimates of the coefficients c_{n0}. From [14], we know that the TBA and CPT $\mathcal{G}$-functions agree in the *massless* case; in table 3 we give the values of c_{00}, c_{10} and c_{20} from CPT and c_{30} from TBA. As can be seen, the extrapolations of c_{00} and c_{10} are really quite good but the TCSA under-estimates the value of c_{20} by about 15% and the value of c_{30} by a similar amount. However, the TCSA estimates are still increasing quite fast with truncation level and would probably agree better on increasing the truncation level.

	TCSA						CPT/TBA
	67 states	81 states	98 states	117 states	140 states	∞ states	
c_{00}	−0.161720	−0.161731	−0.161739	−0.161745	−0.161749	−0.16176	−0.1617535656..
c_{10}	0.997714	0.997731	0.997742	0.997751	0.997758	0.99777	0.9977728216..
c_{20}	−0.044147	−0.044428	−0.044674	−0.044890	−0.045083	−0.046	−0.0525515368..
c_{30}	0.007897	0.007965	0.008024	0.008076	0.008122	0.0084	0.00966359*

Table 3: The coefficients c_{n0} from TCSA, CPT and TBA (denoted by *)

4 The TBA approach to g-functions

The TBA is an alternative to conformal perturbation theory and is characterised by its use of IR scattering data - the bulk scattering matrix of the massive particles, and the reflection factors describing the scattering of the particles off the boundaries.

Exact TBA equations describing the g-function flow for both massive and massless bulk were proposed in [3], following on from earlier work in [15]. The derivation of these equations (which we recall briefly in section 4.2) involved a number of assumptions, but to date only some simple limiting behaviours have been checked. We will perform a more detailed analysis for the Yang-Lee case, which will lead to the conclusion that the equations of [3] do not tell the whole story in every situation.

4.1 The Yang–Lee scattering data

As a massive scattering theory, the Yang–Lee model can be thought of as a reduction of the Sine-Gordon model at coupling constant $8\pi/\gamma = 3/2$ (in the normalisation of [16]). The

bulk spectrum reduces to a single particle (the first Sine-Gordon breather) with two–particle S–matrix [17]

$$S(\theta) = -(1)(2)\ , \quad (x) = \frac{\sinh\left(\frac{\theta}{2} + \frac{i\pi x}{6}\right)}{\sinh\left(\frac{\theta}{2} - \frac{i\pi x}{6}\right)}\ . \tag{4.1}$$

In [4], the boundary reflection factors corresponding to the boundary conditions $\Phi(h)$ and $\mathbb{1}$ discussed in the previous sections were identified as

$$R_{\Phi(h)}(\theta) = R_b(\theta)\ , \quad R_{\mathbb{1}}(\theta) = R_0(\theta)\ , \tag{4.2}$$

where

$$R_b(\theta) = \left(\tfrac{1}{2}\right)\left(\tfrac{3}{2}\right)\left(\tfrac{4}{2}\right)^{-1}\left(S(\theta + i\pi\tfrac{b+3}{6})S(\theta - i\pi\tfrac{b+3}{6})\right)^{-1} \tag{4.3}$$

These reflection factors are special cases of the general Sine-Gordon breather reflection factors proposed in [18] with the parameters η, ϑ of [18, 19] taking the values

$$\frac{2\eta}{\pi} = \pm(\frac{b}{2} + 2)\ , \quad \frac{2i\vartheta}{\pi} = \pm(\frac{b}{2} + 1)\ .$$

In [4] the relation between b and h was conjectured on the basis of numerical fits to be

$$h = -\,|h_c|\,\sin(\pi(b + .5)/5)\,M^{6/5}\ , \quad h_c = -0.685289983(9)\ . \tag{4.4}$$

An exact formula for h_c was also proposed, though no derivation was given; that gap will be filled in section 4.3.5 below. Taking b real gives $|h|<|h_c|M^{6/5}$; to obtain $h<-|h_c|M^{6/5}$ or $h>|h_c|M^{6/5}$ we take $b=-3-i\widehat{b}$ and $b=2+i\widehat{b}$ (with $\widehat{b}$ real) respectively.

The massless limit is obtained by taking $ML = l \to 0$ while keeping $\widetilde{h}$ constant, where

$$\widetilde{h} = hL^{6/5} = -\,|h_c|\,\sin(\tfrac{\pi}{5}(b + \tfrac{1}{2}))\,l^{6/5}\ . \tag{4.5}$$

Since $|h/(h_cM)| \to \infty$ in this limit, b takes the values $-3 - i\widehat{b}$ and $2 + i\widehat{b}$ for $\widetilde{h} > 0$ and $\widetilde{h} < 0$ respectively.

For $\widetilde{h} > 0$, with $b = -3 - i\widehat{b}$, we have $\sin(\frac{\pi}{5}(b + \frac{1}{2})) = -\cosh(\pi\widehat{b}/5)$, and for $\widehat{b} \gg 0$,

$$\widetilde{h} \sim \tfrac{1}{2}\,|h_c|\left(MLe^{\pi\widehat{b}/6}\right)^{6/5}\ . \tag{4.6}$$

Hence the massless limit is $l \to 0$, $\widehat{b} \to +\infty$, $(le^{\pi\widehat{b}/6})$ finite. Substituting $b = -3 - i\widehat{b}$ into (4.3) we find

$$R_{-3-i\widehat{b}}(\theta) = \left(\tfrac{1}{2}\right)\left(\tfrac{3}{2}\right)\left(\tfrac{4}{2}\right)^{-1}\left(S(\theta + \tfrac{\pi\widehat{b}}{6})S(\theta - \tfrac{\pi\widehat{b}}{6})\right)^{-1}\ , \tag{4.7}$$

which is still a pure phase for real θ. Hence, although b is now complex, R_b should still describe a physical reflection process.

For $\widetilde{h} < 0$, $b = 2 + i\widehat{b}$, so $\sin(\frac{\pi}{5}(b + \frac{1}{2})) = \cosh(\pi\widehat{b}/5)$ and for $\widehat{b} \gg 0$,

$$\widetilde{h} \sim -\tfrac{1}{2}\,|h_c|\left(MLe^{\pi\widehat{b}/6}\right)^{6/5}\ . \tag{4.8}$$

Hence the massless limit with $\widetilde{h} < 0$ is $l \to 0$, $\widehat{b} \to +\infty$, $(le^{\pi\widehat{b}/6})$ finite. Substituting $b = 2 + i\widehat{b}$ into (4.3),

$$R_{2+i\widehat{b}}(\theta) = \left(\tfrac{1}{2}\right)\left(\tfrac{3}{2}\right)\left(\tfrac{4}{2}\right)^{-1}\left(S(\theta - \tfrac{\pi\widehat{b}}{6} + i\tfrac{5\pi}{6})S(\theta + \tfrac{\pi\widehat{b}}{6} - i\tfrac{5\pi}{6})\right)^{-1}\ , \tag{4.9}$$

which is not in general a pure phase for real θ. Hence, R_b should not describe a physical reflection process and (in particular) we can no longer expect to find a real spectrum in the IR limit, which was indeed what was found in [4] in the TCSA analysis of the spectrum in the massless case with $\widetilde{h} < 0$.

4.2 The TBA for g-functions

The starting-point for the TBA analysis of [3, 15] was the generalisation of the Bethe-ansatz quantisation equation for particles on a line segment of length $R \to \infty$. Far from the end points, the scattering is characterised by a two-body S-matrix element; information about the reflection of the particles at the end points is encoded in the reflection factors $R_\alpha(\theta)$ and $R_\beta(\theta)$. The main difference with the standard TBA analysis is that the quantity of interest is a sub-leading term (order $1/R$ with respect to the bulk quantities) of the free energy.

The initial assumption is that a particle state can be approximated in the thermodynamic limit ($R \to \infty$) by a distribution of particles in scattering states of given rapidities satisfying self-consistency equations which simultaneously define a density of possible particle states $\rho(\theta)$ and a density of occupied particle states $\rho^r(\theta)$, related by

$$2\pi\rho(\theta) = -2\pi\delta(\theta) + 2MR\cosh\theta + \phi_\alpha(\theta) + \phi_\beta(\theta) - 2\phi(2\theta) + \int_{-\infty}^{\infty} \rho^r(\theta')\phi(\theta-\theta')\mathrm{d}\theta' \ , \quad (4.10)$$

$$\phi(\theta) = -i\frac{\mathrm{d}}{\mathrm{d}\theta}\log S(\theta) \ , \qquad \phi_\alpha(\theta) = -i\frac{\mathrm{d}}{\mathrm{d}\theta}\log R_\alpha(\theta) \ .$$

Assuming that the number of allowed states with effective particle density $\rho^r(\theta)$ is $\mathcal{N}[\rho^r(\theta)]$, one can write the partition function as an integral

$$Z = \sum_{\text{states}} e^{-L\,E} = \int \mathcal{D}[\rho^r(\theta)]\,\mathcal{N}[\rho^r(\theta)]\,e^{-L\,E[\rho^r(\theta)]} \ , \quad (4.11)$$

where the energy of the configuration is $E = \int_0^\infty (M\cosh\theta)\,\rho^r(\theta)\,\mathrm{d}\theta$. The standard TBA method is to calculate $\mathcal{N}[\rho^r(\theta)]$ by taking the number of allowed configurations in the interval $\Delta\theta$ with a fixed number of occupied states $R\rho^r(\theta)\Delta\theta$ to be

$$\frac{(R\rho(\theta)\Delta\theta)!}{(R\rho^r(\theta)\Delta\theta)!(R\rho(\theta)\Delta\theta - R\rho^r(\theta)\Delta\theta)!} \ , \quad (4.12)$$

and replacing the factorials by the two leading terms $\log\Gamma(z) \sim z\log z - z + \ldots$ of Stirling's formula, so that the total number of configurations with a given effective density $\rho^r(\theta)$ is

$$\mathcal{N}[\rho^r(\theta)] \sim \exp\Big[\int_0^\infty (\rho\log\rho - \rho^r\log\rho^r - (\rho-\rho^r)\log(\rho-\rho^r))\,\mathrm{d}\theta\Big] \ . \quad (4.13)$$

We can then calculate Z in the limit $R \to \infty$ by the saddle point method, giving the leading behaviour

$$\log Z \sim -RE_0^{\mathrm{circ}}(L) + \log(g_\alpha(L)\,g_\beta(L)) \ ,$$

where (extending the range of θ by symmetry where necessary and setting $\epsilon = \log(\rho/\rho^r - 1)$)

$$\begin{aligned} E_0^{\rm circ}(L) &= \int_{-\infty}^{\infty} m\cosh\theta\, L(\theta)\,\tfrac{{\rm d}\theta}{2\pi} \\ \log(g_\alpha(L)\, g_\beta(L)) &= \int_{-\infty}^{\infty} \Big(\phi_\alpha(\theta) + \phi_\beta(\theta) - 2\phi(2\theta) - 2\pi\delta(\theta)\Big)\, L(\theta)\,\tfrac{{\rm d}\theta}{4\pi} \end{aligned} \tag{4.14}$$

where $L(\theta) = \log(1 + e^{-\epsilon(\theta)})$ and $\epsilon(\theta)$ solves the equation

$$\epsilon(\theta) = mL\cosh\theta - \int_{-\infty}^{\infty} \phi(\theta - \theta')\, L(\theta')\,\tfrac{{\rm d}\theta'}{2\pi}\ . \tag{4.15}$$

This gives exactly the same result for $E_0^{\rm circ}(L)$ as the usual TBA on a circle [12]. The g-functions are then identified as

$$\log(g_\alpha(L)) \;=\; \textstyle\int_{-\infty}^{\infty} \Big(\,\phi_\alpha(\theta) \;-\; \phi(2\theta) \;-\; \pi\delta(\theta)\,\Big)\, L(\theta)\,\tfrac{{\rm d}\theta}{4\pi} \tag{4.16}$$

There are a number of possible sources of error in this expression. Firstly there are possible corrections from the next-to-leading term $(-\log z/2)$ in Stirling's formula, and secondly from the corrections to the saddle point evaluation of the integral in (4.11). Finally, the initial assumption that the Hilbert space for the model on a line segment can be satisfactorily approximated by scattering states might be wrong. Unfortunately we do not as yet know how account for these effects in a consistent way. In [3] they were formally bypassed by assuming that they give an overall contribution (also appearing in the periodic case) which can be neglected when considering changes in the g-functions. Further problems may arise due to the presence of boundary bound states; again, these were neglected in the above discussion. In section 4.3.1 below the corrections that are necessary for the Yang–Lee model in this case will be found empirically, but a first-principles treatment is still lacking. With these caveats, equations (4.15) and (4.16) form the prediction of [3].

4.3 Properties of the TBA g-functions

From (4.15) and (4.16) it is possible to derive several analytic properties of the TBA g-functions.

In section 4.3.1 we examine possible ambiguities in the g-functions, and give the prescription which we have adopted in this paper. In section 4.3.2, under the assumption that the TBA g-functions are the sum of a term linear in L and a term which is regular in $L^{6/5}$, the coefficient of the linear term is evaluated analytically. This enables us to define the TBA $\mathcal{G}$-functions, which are directly comparable with the TCSA results.

The behaviour of $L(\theta)$ in the UV and IR limits is well understood so it is possible to find the net change in the g-functions along the flow. The g-functions in eqn. (4.16) suffer from ambiguities due to the possibility to change the integration contour, but we show in section 4.3.3 that there are no contours for which the net change in the TBA g-functions agrees with the TCSA result.

In section 4.3.5 we show that the expression for the ratio $\log(g_{\Phi(h(b))}(l)/g_{\mathbb{1}}(l))$ is rather simpler than that for the two g-functions separately, as was also the case in the perturbed

conformal field theory analysis. This enables us to make an expansion in the massless case and obtain the analytic value of h_c defined in eqn. (4.4).

We give some numerical power series fits to the TBA results in section 4.3.6, and find a combination of functions which appears to be regular in $l^{12/5}$.

Finally in section 4.3.7 we discuss the singularities that occur in $g_{\Phi(h)}$ for sufficiently negative $\widehat{h}$ and relate these to the singularity in the ground-state energy on the strip observed in [4].

4.3.1 The contour prescription for the g-functions

If we examine the formula (4.16) for the g-function in a little more detail, we notice a couple of immediate problems. Firstly, the two distinct boundary conditions $\Phi(h(b=0))$ and $\mathbb{1}$ are described by the same reflection factor and hence have the same kernel function ϕ_0, yet have different g-functions. Secondly, ϕ_b describing the $\Phi(h(b))$ boundary condition has poles which are b–dependent and (in particular) cross the real axis for $b=\pm 1$. This means that taking the naive interpretation of (4.16), with the integration contour always along the real axis, will lead to g-functions which are discontinuous at $b=\pm 1$ whereas the physical g-functions should be continuous in b. The resolution of these two problems appears to be that the contour in (4.16) depends on the boundary condition, and in particular is different for the $\mathbb{1}$ and $\Phi(h(b=0))$ boundary conditions. Changing the integration contour will mean encircling some of the poles of ϕ_b, the poles so encircled being called 'active', in analogy with the terminology adopted in [20] in a related context.

The exact choice is, at this stage, a matter of trial and error. In section 4.3.3 we show that there are no choices which will give the same g-functions as the TCSA, but with the following prescription at least the ratios of g-functions agree:

1. The $\mathbb{1}$ boundary condition

   We take $\log(g_{\mathbb{1}})$ to be given by the straightforward application of (4.16), that is

   $$\log(g_{\mathbb{1}}) = \int_{-\infty}^{\infty} \Big(\phi_0(\theta) \,-\, \phi(2\theta) \,-\, \pi\delta(\theta) \Big)\, L(\theta)\, \tfrac{\mathrm{d}\theta}{4\pi} \,,$$

   with the integration contour along the real axis.

2. The $\Phi(h(b))$ boundary condition

   We take $\log(g_{\Phi(h(b))})$ to be given by (4.16) for $-3<b<-1$, that is

   $$\log(g_{\Phi(h(b))}) = \int_{-\infty}^{\infty} \Big(\phi_b(\theta) \,-\, \phi(2\theta) \,-\, \pi\delta(\theta) \Big)\, L(\theta)\, \tfrac{\mathrm{d}\theta}{4\pi} \,, \quad -3<b<-1 \,,$$

   with the integration along the real axis. For all other values of b, it is given by the analytic continuation of this function. In particular, for $\widehat{h}{>}|h_c|$ (i.e. $b{=}{-}3{-}i\widehat{b}$) in the massive case, and for $\widetilde{h}>0$ in the massless, the integration contour may again be taken along the real axis.

The simplest way to derive the continuation of $\log(g_{\Phi(h(b))})$ is to isolate the terms in the integrand which have b–dependent poles and treat these separately. We have

$$\phi_b(\theta) = \phi_0(\theta) - \phi(\theta - i\pi\tfrac{b+3}{6}) - \phi(\theta + i\pi\tfrac{b+3}{6}) \ ,$$

so that for $-3<b<-1$,

$$\log(g_{\Phi(h(b))}) = \log(g_{\mathbb{1}}) - \int_{-\infty}^{\infty} \Big(\phi(\theta - i\pi\tfrac{b+3}{6}) + \phi(\theta + i\pi\tfrac{b+3}{6})\Big) L(\theta)\, \tfrac{\mathrm{d}\theta}{4\pi} \ . \tag{4.17}$$

When the integration contour is along the real axis (but not necessarily otherwise) the two terms in the integral (4.17) give the same contribution, so at least for $-3<b<-1$ we have

$$\log(g_{\Phi(h(b))}) - \log(g_{\mathbb{1}}) \quad = \quad -\int_{-\infty}^{\infty} \phi(\theta - i\pi\tfrac{b+3}{6})\, L(\theta)\, \tfrac{\mathrm{d}\theta}{2\pi} \tag{4.18}$$

The term in the integral $\phi(\theta - i\pi\frac{b+3}{6})$ has poles at

$$\theta = i\pi\tfrac{b-5}{6} + 2n\pi i \ , \quad \theta = i\pi\tfrac{b-1}{6} + 2n\pi i \ , \quad \theta = i\pi\tfrac{b+1}{6} + 2n\pi i \ , \quad \theta = i\pi\tfrac{b+5}{6} + 2n\pi i \ . \tag{4.19}$$

This means that as θ passes from $b<-1$ to $b>-1$, the contour must deform away from the real axis to avoid a discontinuity from the pole at $\theta = i\pi(b+1)/6$, or equivalently the pole at $i\pi(b+1)/6$ is 'active' for $b>-1$, and similarly the pole at $i\pi(b-1)/6$ is 'active' for $b>1$, as shown in figure 14.

Note that the poles that are 'active' are exactly those associated with boundary bound states [4, 21]. It is clear that the transition of a scattering state into a boundary bound state is always associated with a pole in ϕ_α crossing the real axis, and in this case the converse is also true. (Recall that the general interpretation of simple poles can be subtle, and not all correspond to boundary bound states – see [21].) Hence, this seems the natural prescription for the integration contour in the presence of such bound states and it would be interesting to arrive at this result from first principles and check it in further models.

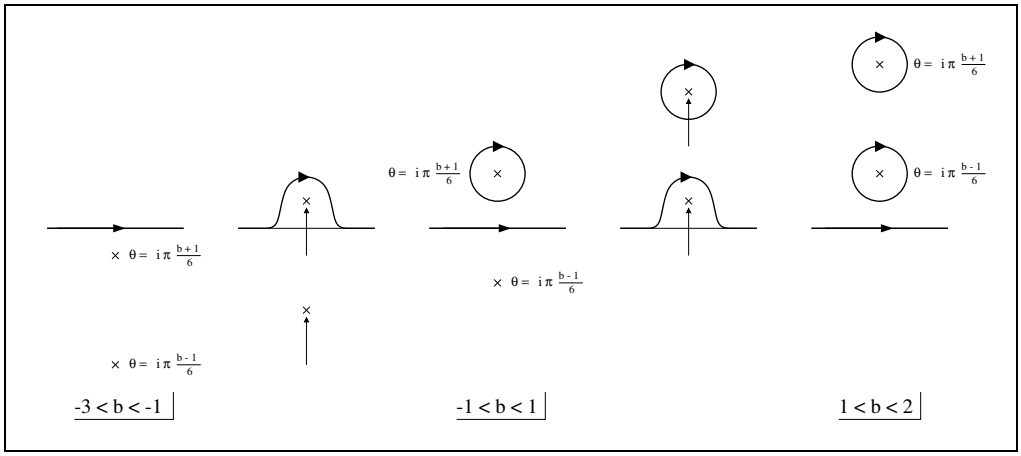

Figure 14: The determination of the contour through the analytic continuation of $\log(g_{\Phi(h(b))})$ from $b<-1$ to $b>1$.

4.3.2 Analytic structure of the TBA g-functions.

We expect the g-functions as evaluated in the TBA to be regular functions of $L^{6/5}$ after the removal of an 'extensive' part, linear in L. Thus they should have the form

$$\log g_\alpha = L f_\alpha + \log \mathcal{G}_\alpha \ .$$

Under this assumption, the coefficient of the linear term can be evaluated analytically as

$$f_\alpha = -\, M \, \frac{\mathrm{d}}{\mathrm{d}l}\, g_\alpha(l) \Big|_{l=0} \ .$$

Al. Zamolodchikov showed in [12] that, in the limit $l \to 0$, $\theta > 0$,

$$L(\theta) \sim L_{\mathrm{kink}}(\theta - \log \tfrac{2}{l})$$

with

$$\int_{-\infty}^{\infty} e^{-\theta}\, \frac{\mathrm{d}L_{\mathrm{kink}}(\theta)}{\mathrm{d}\theta}\, \mathrm{d}\theta = -\frac{\pi}{\sqrt{3}} \ .$$

Substituting this into (4.15) we arrive at

$$f_b^{\mathrm{TBA}} = \left(\tfrac{\sqrt{3}-1}{4} + \sin \tfrac{\pi b}{6} \right) M \ , \tag{4.20}$$

independent of the contour prescription we choose. In the massless limit, using (4.6) we find for $\widetilde{h} > 0$ that

$$f_b^{\mathrm{TBA}} L \sim -\, 2^{-1/6} \left| \widetilde{h}/h_c \right|^{5/6} \ . \tag{4.21}$$

4.3.3 Net change in the TBA g-functions along the flows

Given (4.16), it is straightforward to calculate $\log(g_\alpha)$ in the two limits $L \to 0$ and $L \to \infty$ using the result

$$L(\theta) \to \begin{cases} \log(\frac{1+\sqrt{5}}{2}) \ , & \text{UV}, \\ 0 \ , & \text{IR}. \end{cases} \tag{4.22}$$

While the IR result is simple,

$$\log(\, g_\alpha \,)\Big|_{\mathrm{IR}} = 0 \ , \tag{4.23}$$

the UV limit depends on the choice of integration contour in (4.16). Although we have given above a particular prescription for the contours, no matter which contour is chosen, one *must* end up with

$$\log(\, g_\alpha \,)\Big|_{\mathrm{UV}} = \tfrac{n}{4}\, \log(\tfrac{1+\sqrt{5}}{2}) \ , \quad n \in \mathbb{Z} \ . \tag{4.24}$$

Therefore the most general prediction of (4.14) would be an interpolating flow

$$\log(g_\alpha)\Big|_{\mathrm{UV}} \ - \ \log(g_\alpha)\Big|_{\mathrm{IR}} = \tfrac{n}{4}\, \log(\tfrac{1+\sqrt{5}}{2}) \ , \quad n \in \mathbb{Z} \ . \tag{4.25}$$

There are two distinct physical situations: massless bulk and massive bulk.

1. Massless bulk
   There is a single identifiable massless flow with $\widetilde{h} > 0$, from Φ to $\mathbb{1}$, for which (2.30) gives
   $$\log(g_\Phi) \; - \; \log(g_{\mathbb{1}}) = \log(\tfrac{1+\sqrt{5}}{2}) \; , \tag{4.26}$$
   and which is in agreement with (4.25) for $n = 4$.

2. Massive bulk
   For the massive flows from $\mathbb{1}$ and from $\Phi(h)$ with $\widehat{h}{>}-|h_c|$, g_{UV} are given by conformal field theory, and our expectation that for the massive theory $g|_{IR} = 1$ (already proposed in [4] and well-supported by the TCSA results) leads to the results
   $$\begin{aligned} \log(g_{\mathbb{1}})\Big|_{\rm UV} \; - \; \log(g)\Big|_{\rm IR} &= -\tfrac{1}{4}\log\left|\tfrac{1+\sqrt{5}}{2}\right| - \tfrac{1}{8}\log 5 \; , \\ \log(g_{\Phi(h)})\Big|_{\rm UV} \; - \; \log(g)\Big|_{\rm IR} &= \tfrac{3}{4}\log\left|\tfrac{1+\sqrt{5}}{2}\right| - \tfrac{1}{8}\log 5 \; . \end{aligned} \tag{4.27}$$
   These are in contradiction with (4.25).

Thus we see that the TBA equations (4.15) do not agree with the TCSA even at the level of the overall change in the g-functions without investigating finer detail.

We note however that the ratio $\log(g_\Phi(h)/g_{\mathbb{1}})$ also changes by $\log(\frac{1}{2}(\sqrt{5}+1))$ along a massive flow, so the TBA equations do have the possibility to describe the ratio correctly, and indeed we shall find supporting evidence for this later on.

4.3.4 The relation of the TBA g-functions to the Y–function

Having written the ratio of the g-functions in the form (4.18), we observe that the integral on the right hand side is exactly of the form appearing in the TBA equation determining the pseudo-energy ϵ:

$$\begin{aligned} \log(g_{\Phi(h(b))}) - \log(g_{\mathbb{1}}) &= -\int_{-\infty}^{\infty} \phi(\theta - i\pi\tfrac{b+3}{6})\, L(\theta)\, \tfrac{{\rm d}\theta}{2\pi} \\ &= \epsilon(i\pi\tfrac{b+3}{6}) + l\sin(\tfrac{b\pi}{6}) \; . \end{aligned} \tag{4.28}$$

If we absorb the linear term into the g-functions following (4.20) we obtain exactly the $\mathcal{G}$-functions, so that the g-functions which follow from the TBA equations of [3] predict the particularly simple form for the ratio of the $\mathcal{G}$-functions

$$\log\left(\, \mathcal{G}_{\Phi(h(b))} \,/\, \mathcal{G}_{\mathbb{1}} \,\right) = \epsilon(i\pi\tfrac{b+3}{6}) = \log Y(i\pi\tfrac{b+3}{6}) \; . \tag{4.29}$$

The same result was also obtained in [14] by a different method, but with the restriction to the massless case. Given this, the extension (4.29) to the massive case is perhaps not so surprising, but the derivation via the TBA seems unrelated to the methods of [14]. Just to finish this section, we comment that we have subjected (4.29) to several tests outlined in later sections, all of which support this identity.

4.3.5 The expansion of $\log(\, g_{\Phi(h(b))}(l)\,)$ in the massless limit

The perturbative expansion of $\epsilon(\theta)$ in the massless limit has been found in [14, 22]. If $\epsilon(\theta)$ is normalised so that for large $(l \exp\theta)$ it has the asymptotic behaviour $\epsilon(\theta) \sim \frac{l\,e^\theta}{2}$, then for small $(l \exp\theta)$ it has an expansion

$$\epsilon(\theta) = \log\frac{1+\sqrt{5}}{2} \;+\; C_1\,(l\,e^\theta)^{6/5} \;+\; C_2\,(l\,e^\theta)^{12/5} \;+\; \dots\;,$$

where (from appendix A of [22])

$$C_1 = \frac{2^{-7/5}\pi^{7/5}\Gamma(\frac{1}{5})}{\cos\frac{\pi}{5}\Gamma(\frac{2}{3})\Gamma(\frac{3}{5})^2\Gamma(\frac{4}{5})}\left(\frac{\Gamma(\frac{2}{3})}{\Gamma(\frac{1}{6})}\right)^{6/5}\;, \quad C_2 = \left(\tfrac{1}{\sqrt{5}}-\tfrac{1}{2}\right)C_1^2\;.$$

From perturbed conformal field theory the coefficients in the expansion (3.5) are

$$\log\frac{\mathcal{G}_{\Phi(h)}(0,L)}{\mathcal{G}_{\mathbb{1}}(0,L)} = \log\frac{g_\Phi}{g_{\mathbb{1}}} \;+\; c_{10}\,(hL^{6/5}) \;+\; c_{20}\,(hL^{6/5})^2 \;+\; \dots \tag{4.30}$$

and were found in section 3.2 to be given by (3.27):

$$c_{10} = (2\pi)^{-1/5}5^{1/4}\left|\frac{\Gamma(\frac{2}{5})\Gamma(\frac{6}{5})}{2\cos(\pi/5)\Gamma(\frac{4}{5})^2}\right|^{1/2}\;, \quad c_{20} = \left(\tfrac{1}{\sqrt{5}}-\tfrac{1}{2}\right)(c_{10})^2\;. \tag{4.31}$$

Given that in the massless limit we have

$$\log\frac{\mathcal{G}_{\Phi(h)}(0,L)}{\mathcal{G}_{\mathbb{1}}(0,L)} = \epsilon(\frac{\pi\widehat{b}}{6})\;, \quad hL^{6/5} = -\tfrac{1}{2}\,h_c\,(le^{\pi\widehat{b}/6})^{6/5}\;, \tag{4.32}$$

we deduce that

$$h_c = -\frac{2C_1}{c_{10}} = -\pi^{3/5}\,2^{4/5}\,5^{1/4}\frac{\sin\frac{2\pi}{5}}{(\Gamma(\frac{3}{5})\Gamma(\frac{4}{5}))^{1/2}}\left(\frac{\Gamma(\frac{2}{3})}{\Gamma(\frac{1}{6})}\right)^{6/5} = -0.68528998399118\ldots\;. \tag{4.33}$$

This is in perfect agreement with the numerical result obtained in [4].

4.3.6 Series expansions of ingredients of the TBA expressions

In an attempt to understand better the discrepancies between the TBA results and those from other approaches, we have investigated numerically the various ingredients of the TBA g-functions. The aim was to determine their analytic structure by various power series fits in the variables $x \equiv \lambda L^{12/5}$ and $y \equiv hL^{6/5}$. These results give highly accurate determinations of the first few coefficients, but the accuracy rapidly tails off.

In each case we initially assumed an analytic expansion in $x^{1/2}$ with the addition of possible non-analytic terms of the form $x^{5n/12}$, with the results given in table 4. On the basis of these results we then performed a fit to more restricted functional forms (with fewer non-analytic terms) with the results as in table 5. Finally, we know on theoretical grounds

that $\epsilon(i\pi(b+3)/6)$ has an expansion in x and h and we give the numerical determination of these coefficients in table 6.

$-\frac{1}{2}L(0) \equiv \frac{1}{2}\epsilon(0) - \epsilon(i\pi/3)$	$-0.240605912529803 - 2.2\ 10^{-14}\, x^{5/12} + 0.419185703387\, x^{1/2}$ $-3.\ 10^{-12}\, x^{10/12} - 0.26930751\, x - 3.6\ 10^{-8}\, x^{15/12} + 0.0120551\, x^{3/2}$ $-1.\ 10^{-7}\, x^{20/12} + 0.07138\, x^2 - 2.5\ 10^{-5}\, x^{25/12} - 0.0096\, x^{5/2} + \ldots$
$L(\frac{i\pi}{6})$	$0.481211825059603 - 4.\ 10^{-14}\, x^{5/12} - 0.67825671567\, x^{1/2}$ $-9.1\ 10^{-13}\, x^{10/12} + 0.308598962\, x - 7.\ 10^{-8}\, x^{15/12} + 0.05575394\, x^{3/2}$ $-1.3\ 10^{-7}\, x^{20/12} - 0.08108\, x^2 - 2.6\ 10^{-5}\, x^{25/12} - 0.023\, x^{5/2} + \ldots$
$-\int_{-\infty}^{\infty} \phi(2\theta)\, L(\theta)\, \frac{d\theta}{2\pi}$	$0.240605912529 - 7.3\ 10^{-10}\, x^{5/12} - 0.67825671\, x^{1/2}$ $+0.8102843\, x^{10/12} - 0.33287\, x - 0.0002\, x^{15/12}$ $+0.062\, x^{3/2} - 0.045\, x^{20/12} + \ldots$
$\int_{-\infty}^{\infty} \phi_0(\theta)\, L(\theta)\, \frac{d\theta}{2\pi}$	$-0.4812118250596 + 0.967384888\, x^{5/12} - 4.3\ 10^{-9}\, x^{1/2}$ $-0.8102843\, x^{10/12} + 0.20572x + 0.00026x^{15/12}$ $+\ldots$
$\int_{-\infty}^{\infty} (\phi_0(\theta) - \phi(2\theta))\, L(\theta)\, \frac{d\theta}{2\pi}$	$-0.2406059125298 + 0.96738488748\, x^{5/12} - 0.6782567157\, x^{1/2}$ $+6.\ 10^{-9}\, x^{10/12} - 0.1271498\, x + 5.\ 10^{-7}\, x^{15/12} + 0.055748\, x^{3/2}$ $+9.\ 10^{-6}\, x^{20/12} - 0.02350\, x^2 + 0.00004\, x^{25/12} + \ldots$

Table 4: the results of inital fits to the TBA data

$-\frac{1}{2}L(0)$	$-0.240605912529802 + 0.4191857033888\, x^{1/2} - 0.269307520\, x$ $+0.0120552\, x^{3/2} + 0.07138\, x^2 - 0.0096\, x^{5/2}$ $+\ldots$
$L(\frac{i\pi}{6})$	$0.481211825059603 - 0.678256715680\, x^{1/2} + 0.30859896278\, x$ $+0.055753953\, x^{3/2} - 0.081082\, x^2 - 0.023\, x^{5/2}$ $+\ldots$
$-\int_{-\infty}^{\infty} \phi(2\theta)\, L(\theta)\, \frac{d\theta}{2\pi}$	$0.240605912529805 - 0.67825671\, x^{1/2} + 0.8102848\, x^{10/12}$ $-0.332875\, x - 0.00020\, x^{15/12} + 0.0615\, x^{3/2}$ $-0.043\, x^{20/12} + \ldots$
$\int_{-\infty}^{\infty} \phi_0(\theta)\, L(\theta)\, \frac{d\theta}{2\pi}$	$-0.481211825059593 + 0.96738488736\, x^{5/12} - 0.8102849\, x^{10/12}$ $+0.20572\, x + 0.00021\, x^{15/12} - 0.0060\, x^{3/2} + 0.043\, x^{20/12}$ $+\ldots$
$\int_{-\infty}^{\infty} (\phi_0(\theta) - \phi(2\theta))\, L(\theta)\, \frac{d\theta}{2\pi}$	$-0.240605912529802 + 0.9673848874698\, x^{5/12}$ $-0.6782567156814\, x^{1/2} - 0.127149765\, x + 0.05575395\, x^{3/2}$ $+0.023491\, x^2 - 0.020\, x^{5/2} + \ldots$

Table 5: the results of more restricted fits to the TBA data

$\varepsilon(\imath\pi\frac{b+3}{6}) = mL\sin\frac{\pi b}{6} - \int_{-\infty}^{\infty}\phi(i\pi\frac{b+3}{6}-\theta)L(\theta)\,\mathrm{d}\theta/(2\pi)$
$0.48121182508 + 0.332882394\,x - 0.09242282\,x^2 + 0.040463\,x^3 - 0.02047\,x^4 + 0.0104\,x^5 - 0.00385\,x^6$
$+0.9977728224\,y - 0.086482609\,xy + 0.03812851\,x^2y - 0.01991664\,x^3y + 0.010374\,x^4y - 0.00377\,x^5y$
$-0.052551643\,y^2 + 0.02553410\,xy^2 - 0.0148490\,x^2y^2 + 0.008372\,x^3y^2 - 0.003206\,x^4y^2$
$+0.00966359\,y^3 - 0.0076724\,xy^3 + 0.005150\,x^2y^3 - 0.00225\,x^3y^3$
$-0.0021742\,y^4 + 0.002199\,xy^4 - 0.00119\,x^2y^4$
$+0.000563\,y^5 - 0.00046\,xy^5 - 0.00016\,y^6$

Table 6: numerical fit to the expansion of ϵ

We immediately notice that with the contour prescription of section 4.3.1, not only does $g_{\mathbb{1}}$ not have the correct net overall change, but neither is $\mathcal{G}_{\mathbb{1}}$ a pure power series in x (λ). Even sacrificing universality, with the lack of such a basic property there is no hope to identify this quantity with a properly defined g-function.

However, we observe that it is possible to find a function which has a regular expansion in x from the various ingredients of the TBA. If we drop the term $-L(0)/2$ (which was introduced in [3] to account for the absence of a zero-momentum single particle state on the strip), and further, instead of running the contour on the real axis, we instead also encircle the singularity of ϕ_0 at $\theta = i\pi/6$ clockwise to pick up an extra contribution $-L(i\pi/6) \equiv -\epsilon(i\pi/2)$, we arrive at the function

$$\int_{-\infty}^{\infty}(\phi_0(\theta) - \phi(2\theta))\,L(\theta)\,\frac{\mathrm{d}\theta}{2\pi} - \epsilon(\tfrac{i\pi}{2})\ ,$$

for which we find the expansion

$$\begin{aligned}&-0.7218177375894 + 0.967384887468\,x^{5/12} + 2.\ 10^{-13}\,x^{1/2} - 0.435748727\,x\\ &\quad + 6.\ 10^{-10}\,x^{3/2} + 0.10457\,x^2 + 0.004\,x^{5/2}\end{aligned}$$

which has (within our accuracy) better prospects of being a purely analytic function of x, plus a term in $x^{5/12}$ which we can identify as $(\sqrt{3}-1)\kappa\,x^{5/12}/2 = (\sqrt{3}-1)l/2$.

To conclude, the g-functions predicted by the TBA equations of [3] do not match the quantities derived perturbatively in this paper, nor do they have the expected analytic properties. Although we have partial evidence that the latter problem could be overcome with an ad-hoc contour prescription, at the present stage of our understanding we have no definite justification for the above-mentioned discrepancies.

4.3.7 Singularities for $\widehat{h} < -|h_c|$

In section 4.3.1, we made the following identification in the case of massive bulk:

$$\log(g_{\Phi(h(b))}) - \log(g_{\mathbb{1}}) = \epsilon(i\pi\tfrac{b+3}{6}) + l\sin(\tfrac{b\pi}{6})\ . \tag{4.34}$$

The TCSA analysis in [4] revealed the existence of a critical value of $hM^{-6/5}$, in the range $-0{\cdot}8$ to $-0{\cdot}6$, for which $\log(g_{\Phi(h(b))}g_{\mathbb{1}})$ diverges — this was signalled by a pole in a rational fit to the g-function. Furthermore, the ground state energy on the strip has a square–root

singularity at some real value of r for $hM^{-6/5} < h_c M^{-6/5} = -0.68529..$ (see section 6 of [4]). This led us to the conjecture that the singularities in the two quantities occur at the same critical threshold $h_c M^{-6/5}$. Armed with relation (4.34) we can now prove this. First note that the quantity $Y(\theta, r) = \exp(\epsilon(\theta, r))$ is entire in θ; further, for $r \equiv RM$ real, it has zeroes on the line $\mathrm{Im}\,\theta = 5\pi/6$ (or equivalently $\mathrm{Im}\,\theta = -5\pi/6$), arranged symmetrically about the imaginary axis. While their exact locations θ_n are not known, for large r a good approximation is $\sinh(\mathrm{Re}\,\theta_n) = \pm\pi(2n+1)/r$ $(n = 0, 1, 2, \ldots)$. Hence as r grows these zeroes move towards $\mathrm{Re}\,\theta = 0$.

Suppose now that $\mathrm{Re}\,b = 2$ so that the value $\theta(b) = i\pi\frac{b+3}{6}$ relevant for (4.34) lies on the line $\mathrm{Im}\,\theta = 5\pi/6$. As r increases, the zeroes θ_n of Y move along the line $\mathrm{Im}\,\theta = 5\pi/6$ and at some critical value $r_c(b)$ one will pass through $\theta(b)$, so that $Y(\theta(b), r_c(b)) = 0$. This confirms the presence of logarithmic singularities in (4.34), fixes the critical threshold at b=2 and proves (through eq. (4.4)) the above mentioned conjecture. A similar analysis shows that logarithmic singularities appear in the massless $h < 0$ case too.

5 Comparison of TBA, CPT and TCSA results

Firstly, it is a consequence of [14] that the TBA and CPT methods give the same answer for the $\mathcal{G}$-function along the massless flow. This is borne out by the comparison of our TCSA data with the TBA. However, we find disagreement between the TCSA and TBA predictions for the massive flows.

On general grounds we showed in section 3 that the perturbative parts of the g-functions, denoted by $\mathcal{G}$-functions, should have a series expansion for small L in $L^{6/5}$. However, when we try to combine the power series expansions for the various ingredients given in section 4.3.6 we see that the $\mathcal{G}$-functions predicted by the massive TBA equations of [3] do not have the correct behaviour. This is compounded by the fact that in the massive case the net change in the g-functions does not agree with the CFT predictions. This leads us to our conclusion that the g-functions and $\mathcal{G}$-functions given by the massive TBA equations of [3] do not agree with those obtained viewing the theory as a perturbed conformal field theory.

One of the most natural sources of this discrepancy is from a neglected sub-leading term in the saddle point evaluation of $\log Z$, but we have not been able to calculate such a term. What is clear is that the discrepancy between the TBA and CPT calculations of the g-functions is independent of the boundary conditions. This is consistent with our observations in tables 7 and 3 that the first few coefficients in the power series expansions obtained from the TBA and TCSA for the *ratio* of $\mathcal{G}$-functions, $\log(\mathcal{G}_{\Phi(h)}/\mathcal{G}_{\mathbb{1}})$ do agree and that the extensive free-energy terms (the linear behaviour of the $\mathcal{G}$-functions for large L) are also the same in the TBA and TCSA results.

	TCSA (∞ states)	TBA	exact
$c_{01} - d_1$	0.332	0.332882394	0.332882407..
$c_{02} - d_2$	−0.092	−0.09242282	—
$c_{03} - d_3$	0.039	0.040463	—
$c_{03} - d_3$	−0.02	−0.02047	—

Table 7: The coefficients $(c_{0n} - d_n)$ from TCSA, TBA and CPT

As further evidence we show in figure 15 the TCSA and TBA estimates for the ratio of $g_{b=-1.1}$ and $g_{b=-1.2}$.

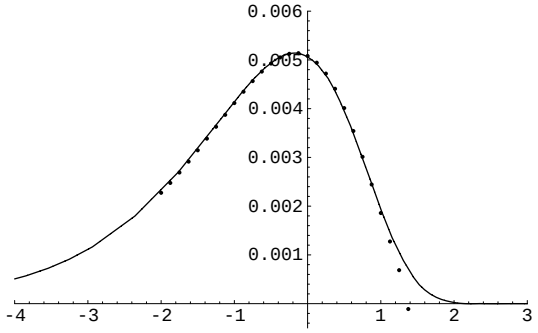

Figure 15: The difference $\log(g_{b=-1.1}) - \log(g_{b=-1.2})$ vs. $\log l$ for the massive YL model. The solid line is the TBA result and the points are from the TCSA to 117 states.

6 Conclusions

We have investigated the relation between the g-functions proposed on the basis of a TBA analysis in [3] and those obtained from perturbed conformal field theory.

We found that the massless case is correctly described by the TBA g-functions (up to an overall constant) but that the massive case is not. However, in all cases, the ratios of $\mathcal{G}$-functions for different boundary conditions of the same model are correctly predicted by the TBA. A consequence of the TBA proposal of [3] is that this ratio of perturbative $\mathcal{G}$-functions should satisfy

$$\frac{\mathcal{G}_{\Phi(h(b))}}{\mathcal{G}_{\mathbb{1}}} = Y(i\pi\tfrac{b+3}{6}) \; . \tag{6.1}$$

This relation is already contained in the results of [14] in the *massless* case, but the derivation there seems rather different to ours. We have tested (6.1) in the massive case in two ways: we have compared the power series expansions from fits to the TBA data to the perturbed conformal field theory and TCSA calculations of these expressions; we have further compared the ratio of $\mathcal{G}$-functions directly over a range of l using the TBA and TCSA. Both tests support (6.1).

We have also found strong support from the TCSA for the correctness of the TBA calculation of the 'extensive' boundary free energy f_α.

To summarise, we have found strong evidence for the relation

$$g_\alpha^{\mathrm{CFT}}(l) = g_\alpha^{\mathrm{TBA}}(l) + k(l) \; ,$$

where $k(l)$ is an (unknown) function of l vanishing at $l = \infty$, and which is independent of the boundary conditions, and where g_α^{TBA} is the function which results from the equations of [3], analytically continued from the massless regime. In section 4.3.6 we further conjectured that

$$g_\alpha^{\mathrm{CFT}}(l) = g_\alpha^{\mathrm{TBA}}(l) + \tfrac{1}{4}L(0) - \tfrac{1}{2}\epsilon(\tfrac{i\pi}{2}) + \widetilde{k}(l) \; ,$$

where $\widetilde{k}(l)$ is an (unknown) regular function of $l^{12/5}$ vanishing at $l = \infty$, and which is independent of the boundary conditions, and where again $g_\alpha^{\rm TBA}$ is analytically continued from the massless regime. This is just the sort of relation that would arise if the TBA prediction of [3] has neglected some corrections arising as next-to-leading order terms in the saddle-point evaluation of the path integral giving the partition function. As yet we have not been able to check this possibility.

One of the unresolved problems we encountered was the correct contour prescription when the kernel function ϕ_α contained parameter-dependent poles. The result we found in section 4.3.1 is that it is consistent to take the contour to encircle those poles which correspond to boundary bound states. As mentioned there, it will be interesting to arrive at this result from first principles and check it in further models. However it is clear that no change in this contour prescription can correct the TBA g-functions of [3] which will still have the wrong net overall change in g along the massive flows.

We should also like to point out that the g-functions we obtain to not satisfy the 'g–theorem', but since this model is non-unitary that is perhaps no surprise.

Another point to mention is that, in the massive case, $Y(\theta, r)$ possesses square-root singularities in the parameter r. These singularities lead to branch-points connecting the bulk vacuum energy to excited states [20], for which the Y–functions are described by so-called excited state TBA equations [20, 22]. It would be nice to understand the role of these "excited" branches of Y in the framework of boundary theories, especially in the light of the result 6.1 From the discussion in [22] it seems clear that in the *massless* case the excited branches Y_n give the coefficients of the boundary state expanded in the eigenstates of the conformal field theory conserved quantities, i.e. if $\langle\, \psi_n \,|$ is the n-th excited state of the conformal field theory and $|\, \Phi(h) \,\rangle$ is the boundary state for the massless perturbation of the boundary Φ, then (cf. eq. (4.32))

$$\langle\, \psi_0 \,|\, \Phi(h) \,\rangle = \langle\, \varphi \,|\, \Phi(h) \,\rangle = Y(\tfrac{\pi \widehat{b}}{6}) \langle\, \varphi \,|\, \mathbb{1} \,\rangle \;, \quad \langle\, \psi_n \,|\, \Phi(h) \,\rangle = Y_n(\tfrac{\pi \widehat{b}}{6}) \langle\, \psi_n \,|\, \mathbb{1} \,\rangle \;.$$

Quite how this generalises to the massive model is not yet clear, but for the ground state we have given strong evidence for

$$\frac{\langle\, \Omega \,|\, \Phi(h) \,\rangle}{\langle\, \Omega \,|\, \mathbb{1} \,\rangle} = Y(i\pi \tfrac{b+3}{6})$$

so it is reasonable to suppose that, by analytic continuation in λ, the same should remain true in general, i.e.

$$\frac{\langle\, \psi_n \,|\, \Phi(h) \,\rangle}{\langle\, \psi_n \,|\, \mathbb{1} \,\rangle} = Y_n(i\pi \tfrac{b+3}{6}) \;.$$

Some preliminary numerical and CPT checks support this conjecture.

The TBA for g-functions was used in a recent paper by Lesage et al. [23], as part of an analysis of boundary flows in minimal models. In the light of the doubts raised above, it is possible that some of their conclusions for cases where the bulk as well as the boundary is perturbed should now be re-examined. However, since we have deliberately focussed on just one model in this paper, we will leave these questions for future work.

Al. Zamolodchikov has recently found the exact correspondence between the UV and IR parameters in the Sine-Gordon model based on calculations of the extensive term f_α from the

TBA g-functions and from exact results for the expectation value of the boundary field [24]. Since the Yang–Lee model can be viewed as one special case of the Sine-Gordon model, his results should include our result relating h, M and b, summarised in equations (4.4) and (4.33), as a special case. So far, his results are not directly comparable with ours, but they are of the same functional form, only h_c not being identified. A complete comparison between his results and ours would require the relation between the normalisations of the fields in the two approaches, and this has yet to be found.

Acknowledgements — The work was supported in part by a TMR grant of the European Commission, contract reference ERBFMRXCT960012, in part by a NATO grant, number CRG950751, and in part by an EPSRC grant GR/K30667. PED and GMTW thank the EPSRC for Advanced Fellowships, and RT thanks the Universiteit van Amsterdam for a post-doctoral fellowship. IR thanks the DAAD, EPSRC and KCL for financial support.

GMTW would like to thank J.-B. Zuber for numerous discussions; PED and GMTW would like to thank Al. Zamolodchikov for discussions of these results and those of [24].

References

[1] J.L. Cardy, *Boundary conditions, fusion rules and the Verlinde formula*, Nucl. Phys. **B324** (1989) 581–596.

[2] I. Affleck and A.W.W. Ludwig, *Universal noninteger "Ground-State Degeneracy" in critical quantum systems*, Phys. Rev. Lett. **67** (1991) 161–164.

[3] A. LeClair, G. Mussardo, H. Saleur and S. Skorik, *Boundary energy and boundary states in integrable quantum field theories*, Nucl. Phys. **B453** (1995) 581–618, `hep-th/9503227.`

[4] P. Dorey, A. Pocklington, R. Tateo and G. Watts, *TBA and TCSA with boundaries and excited states*, Nucl. Phys. **B525** (1998) 641–663, `hep-th/9712197.`

[5] R.E. Behrend, P.A. Pearce, V.B. Petkova and J.-B. Zuber, *Boundary Conditions in Rational Conformal Field Theories,* `hep-th/9908036.`

[6] I. Runkel and G. Watts, in preparation.

[7] J.L. Cardy and D.C. Lewellen, *Bulk and boundary operators in conformal field theory*, Phys. Lett. **B259** (1991) 274–278.

[8] D.C. Lewellen, *Sewing constraints for conformal field theories on surfaces with boundaries*, Nucl. Phys. **B372** (1992) 654–682.

[9] I. Runkel, *Boundary structure constants for the A-series Virasoro minimal models*, Nucl. Phys. **B549** (1999) 563-578, `hep-th/9811178.`

[10] J.L. Cardy and I. Peschel, *Finite size dependence of the free energy in two-dimensional critical systems*, Nucl. Phys. **B300** (1988) 377–392

[11] V.P. Yurov and Al.B. Zamolodchikov, *Truncated conformal space approach to the scaling Lee-Yang model,* Int. J. Mod. Phys. **A5** (1990) 3221-3246.

[12] Al.B. Zamolodchikov, *Thermodynamic Bethe Ansatz in Relativistic Models. Scaling 3-state Potts and Lee-Yang Models*, Nucl. Phys. **B342** (1990) 695-720.

[13] Al.B. Zamolodchikov, Mass scale in sine-Gordon model and its reductions, Int. J. Mod. Phys. **A10** (1995) 1125-1150.

[14] V.V. Bazhanov, S.L. Lukyanov and A.B. Zamolodchikov, *Integrable Structure of Conformal Field Theory, Quantum KdV Theory and Thermodynamic Bethe Ansatz*, Commun. Math. Phys. **177** (1996) 381–398, `hep-th/9412229`.

[15] P. Fendley and H. Saleur, *Deriving boundary S matrices*, Nucl. Phys. **B428** (1994) 681–693, `hep-th/9402045`.

[16] A.B. Zamolodchikov and Al.B. Zamolodchikov, *Factorized S–matrices in two dimensions as the exact solutions of certain relativistic quantum field theory models,* Ann. Phys. **120** (1979) 253–291.

[17] J.L. Cardy and G.Mussardo, *S matrix of the Yang-Lee edge singularity in two dimensions*, Phys. Lett. **B225** (1989) 275–278.

[18] S. Ghoshal, Boundary state boundary S-matrix of the sine-Gordon model, Int. J. Mod. Phys. **A9** (1994) 4801–4810, `hep-th/9310188`.

[19] S. Ghoshal and A.B. Zamolodchikov, *Boundary S matrix and boundary state in two-dimensional integrable quantum field theory*, Int. J. Mod. Phys. **A9** (1994) 3841-3886, `hep-th/9306002`.

[20] P. Dorey and R. Tateo, Excited states by analytic continuation of TBA equations, Nucl. Phys. **B482** (1996) 639–659, `hep-th/9607167`;
— Excited states in some simple perturbed conformal field theories, Nucl. Phys. **B489** (1998) 575-623, `hep-th/9706140`.

[21] P. Dorey, R. Tateo and G.M.T. Watts, *Generalisations of the Coleman-Thun mechanism and boundary reflection factors*, Phys. Lett. **B448** (1999) 249-256, `hep-th/9810098`.

[22] V.V. Bazhanov, S.L. Lukyanov and A.B. Zamolodchikov, Integrable quantum field theories in finite volume: excited state energies, Nucl. Phys. **B489** (1997) 487–531, `hep-th/9607099`.

[23] F. Lesage, H. Saleur and P. Simonetti, *Boundary flows in minimal models*, Phys. Lett. **B427** (1998) 85–92, `hep-th/9802061`.

[24] Al.B. Zamolodchikov, talk at the 4th Bologna workshop on conformal and integrable models, June 30 - July 3, 1999 [unpublished].